

# Topological fluid mechanics of point vortex motions

**Philip Boyland**<sup>1</sup>, Department of Mathematics, University of Florida, 358 Little Hall, Gainesville, FL 32611-8105

**Mark Stremler** and **Hassan Aref**, Department of Theoretical and Applied Mechanics, University of Illinois, 104 South Wright Street, Urbana, IL 61801

**Abstract:** Topological techniques are used to study the motions of systems of point vortices in the infinite plane, in singly-periodic arrays, and in doubly-periodic lattices. The reduction of each system using its symmetries is described in detail. Restricting to three vortices with zero net circulation, each reduced system is described by a one degree of freedom Hamiltonian. The phase portrait of this reduced system is subdivided into regimes using the separatrix motions, and a braid representing the topology of all vortex motions in each regime is computed. This braid also describes the isotopy class of the advection homeomorphism induced by the vortex motion. The Thurston-Nielsen theory is then used to analyse these isotopy classes, and in certain cases strong conclusions about the dynamics of the advection can be made.

## §1 Introduction.

The modelling of incompressible flow at high Reynolds number as a potential flow with embedded vortices has repeatedly proven useful both for analytical and numerical purposes. The subject has inspired numerous reviews, each stressing different aspects of the field. The articles by Aref [Af1], Chorin [C1-3], Leonard [L], Majda [Mj], Moffatt & Tsinober [MFT], Pullin & Saffman [PS], Saffman & Baker [SB], Saffman [S], Sarpkaya [Srp], Shariff & Leonard [SL], and Zabusky [Z] provide a representative sample. We are concerned here with the further simplification of modelling a two-dimensional flow by a finite collection of point vortices. While this system is admittedly highly idealised, it has found application and, to some extent, experimental verification starting with von Kármán's analysis in 1912 of the instability of the vortex street wake behind a cylinder and Onsager's 1949 explanation of the emergence of large coherent vortices in two-dimensional flow through an 'inverse cascade' of energy. (See the literature cited for further details.)

In this paper we study the evolution of three kinds of point vortex systems, in the infinite plane, in singly-periodic arrays, and in doubly-periodic lattices. An array of point vortices is useful in modelling flows in shear layers, wakes and jets. The motivation for studying vortex lattices comes from the problem of two-dimensional turbulence, a paradigm of atmospheric and oceanographic flows, and to a lesser extent from the study of vortex patterns formed in superfluid Helium.

Kirchhoff recognised that the evolution of  $N$  point vortices could be formulated within the framework of classical mechanics as an  $N$ -degree of freedom Hamiltonian system. In many ways point vortices are the fluid mechanical analog of point masses evolving under the mutual interaction of Newtonian gravity. As with the  $N$ -body problem, point vortex systems have continuous symmetries that give rise to integrals of motion. In the case of zero net circulation (a case of considerable physical interest), the two integrals arising from translation invariance are in involution. Thus for three vortices, the Hamiltonian system is completely integrable.

---

<sup>1</sup> To whom correspondence should be addressed: boyland@math.ufl.edu

Fixing a value of these integrals and factoring out by the corresponding group action gives rise to a new Hamiltonian system with two less degrees of freedom. For three vortex systems, this process of Jacobi-Poincaré reduction yields a single degree of freedom system. Vortex arrays and lattices also have a discrete symmetry coming from the array or lattice structure. For rational circulation ratios these result in a discrete symmetry of the reduced system whose phase space is consequently a cylinder or torus. Symmetries and reduction are explained in detail in §3.

Since the reduction is accomplished by factoring out the translational invariance, trajectories in the reduced system describe the evolution of the shape and orientation of the triangle spanned by the three vortices. Because the reduced system has one degree of freedom the generic bounded orbit is periodic. This implies that the corresponding triangle of vortices resumes its shape and orientation after one period. However, the triangle may be translated. This translation vector is a dynamic phase of the type that arises when the evolution of a full system is reconstructed from a periodic trajectory of a reduced system. (For a general introduction to reduction and dynamic phases see [MZ1] and [MZ2]. Further references are given in §3.)

Having performed the reduction on a three-vortex system, the dynamics of the vortices can be understood by analysing a one degree of freedom Hamiltonian system (see [Af2], [AS1] and [SA]). In such systems the phase portrait is organised by the saddle points and the connections between them, known as separatrices (see Figures 3.1 and 3.2). For vortices the reduced Hamiltonian will also have singularities or poles arising from collisions, or more properly, from the superposition of pairs of vortices as collisions do not occur when there is zero total circulation. The separatrices naturally divide the phase space into regions (called regimes in this paper) in which one would expect the corresponding fluid motions to share certain dynamical characteristics. These characteristics are topological and are precisely described using Artin's braid group. The assignment of a braid to a vortex motion is accomplished by visualising the vortex motion in a three dimensional space-time with the two space directions in the usual  $xy$ -plane and time going upwards. The motion in the vortex frame is periodic, and so the strands representing the motions in this frame have the same initial and final position. The translation into a mathematical braid in Artin's group is accomplished by projecting onto a fixed plane which is orthogonal to the  $xy$ -plane. This construction is described in §4 where it is shown that all the vortex motions arising from the same regime are described by the same braid. Examples in the infinite plane and in an array are worked out in detail.

As a Hamiltonian system the vortex evolution takes place in a  $2n$ -dimensional phase space. However, from a fluid mechanical perspective it is much more natural to view the motion as  $N$  trajectories in the plane (or the cylinder or torus in the array and lattice cases). Since the vortices carry concentrated vorticity, they generate a velocity field in the surrounding fluid. The evolution of passive tracer particles in this velocity field is called advection. In mathematical terms, advection is the evolution according to solutions of the differential equation corresponding to the vector field of velocities. Returning to the case of three vortices with zero net circulation, we pass to the vortex frame to eliminate the dynamic phase and so obtain a periodic motion of the vortices. In this frame the vortices generate a periodic velocity field, and so we define the *advection homeomorphism* as the Poincaré map obtained by advecting for one period in this frame. Thus iterates of the advection homeomorphism describe the dynamics of advection in the vortex frame (see §6.1).

In §5.1 the braid of a regime is connected to the corresponding advection homeomorphisms using the notion of isotopy. Two homeomorphisms are isotopic if one can be obtained from the other by a continuous deformation. In addition to its role as a description of the topology of a periodic motion of  $N$  points in the plane, a braid on  $N$  strands also naturally describes an isotopy class of homeomorphisms on the  $N$ -punctured plane. Since all the motions in a regime have the same braid, they all generate isotopic advection homeomorphisms. This knowledge is then applied using Thurston-Nielsen theory of surface homeomorphisms.

The Thurston-Nielsen theory (described in §5.2 and §5.3) contains a classification theorem for isotopy classes of surface homeomorphisms. In the case of a pseudoAnosov class the theory gives dynamical behaviour that must be present in every homeomorphism in the isotopy class. This information includes a lower bound for such quantities and structures as the growth rate of the number of periodic orbit points as the period grows, the topological entropy, the growth rate of the length of topologically nontrivial material lines, and the topology of invariant manifold templates. In particular, any homeomorphism in a pA class will be chaotic under any of the usual definitions of the word. For three vortices in the plane with zero net circulation, the advection homeomorphisms are never in pseudoAnosov classes, but for vortex arrays and lattices, pseudoAnosov classes are common. Examples are discussed in detail in §6.2 and §6.3.

Because we believe the methods described in this paper have general applicability, an effort has been made to make the paper accessible to a general scientific reader, perhaps lacking expertise in topology and/or fluid mechanics. A fair amount of expository material has been included. In certain cases (eg. §4.1 and §5.1) basic material needed in a form not available in the literature is described in some mathematical detail. The reader may prefer to skip these sections in a first reading.

## §2 Equations of motion and Hamiltonians.

We shall be considering the evolution of three types of systems of vortices: finite collections in the infinite plane, singly-periodic arrays and doubly-periodic lattices. The names “array” and “lattice” will be reserved for the singly- and doubly-periodic systems, respectively. Both real and complex notation will be used for points in the plane with  $z = x + iy$  in all cases. A singly-periodic array of  $N$  vortices of period (or width)  $L$  is a collection of vortices in the plane with exactly  $N$  vortices in each vertical strip of width  $L$  and if there is a vortex at position given by a complex number  $z_\alpha$  there is also one at  $z_\alpha + nL$  for all integers  $n$ . The definition of a vortex lattice requires a pair of linearly independent complex numbers  $\omega_1$  and  $\omega_2$  (the *half-periods*) that determine the double-periodicity. A doubly-periodic lattice of  $N$  vortices with lattice structure generated by  $\omega_1$  and  $\omega_2$  is a collection of point vortices that has exactly  $N$  vortices in each fundamental parallelogram determined by  $2\omega_1$  and  $2\omega_2$ , and if there is a vortex at position  $z_\alpha$  there is also one at  $z_\alpha + n_1 2\omega_1 + n_2 2\omega_2$  for all integers  $n_1$  and  $n_2$ . Eventually we shall describe vortex arrays or lattices by singly- or doubly-periodic coordinates, or equivalently, as  $N$  vortices on a cylinder or torus. However, initially the arrays or lattices are specified by a collection of  $N$  distinguished points. Thus, for example,  $(z_1 + L, z_2, z_3)$  represents a different array than  $(z_1, z_2, z_3)$ . Note also that our definition of lattice requires that it maintain the same periodicity for all time, so a uniformly rotating system is not a lattice in our sense.

**§2.1 Equations of motion for the vortex systems.** The  $\alpha^{th}$  point vortex has a constant circulation given by the real number  $\Gamma_\alpha$  and a position at time  $t$  given by the complex number

$z_\alpha(t)$ . Using an asterisk denotes the complex conjugate, the  $N$  differential equations that describe the evolution of the vortex systems are

$$\frac{dz_\alpha^*}{dt} = \frac{1}{2\pi i} \sum_{\beta \neq \alpha} \Gamma_\beta \phi_{\mathcal{X}}(z_\alpha - z_\beta) \quad (2.1)$$

for  $\alpha = 1, \dots, N$ . Using  $\mathcal{X} = \mathcal{P}$  for the infinite plane,  $\mathcal{X} = \mathcal{A}$  for arrays, and  $\mathcal{X} = \mathcal{L}$  for lattices, the complex-valued function  $\phi_{\mathcal{X}}$  in the various cases is

$$\begin{aligned} \phi_{\mathcal{P}}(z) &= \frac{1}{z} \\ \phi_{\mathcal{A}}(z) &= \frac{\pi}{L} \cot\left(\frac{\pi}{L}z\right) \\ \phi_{\mathcal{L}}(z) &= \zeta(z) + \delta z - \frac{\pi}{\Delta} z^* \end{aligned} \quad (2.2)$$

where in the lattice case,  $\zeta(z) = \zeta(z; \omega_1, \omega_2)$  is the Weierstrass zeta function,  $\Delta$  is the area of a fundamental parallelogram, and  $\delta = \frac{\pi}{\Delta} - \frac{\zeta(\omega_1)}{\omega_1}$ . Note that in each case the function  $\phi$  is odd and has the required periodicity;  $\phi_{\mathcal{L}}(z + nL) = \phi_{\mathcal{L}}(z)$  and  $\phi_{\mathcal{A}}(z + 2n_1\omega_1 + 2n_2\omega_2) = \phi_{\mathcal{A}}(z)$  (the latter identity uses the Legendre relation for the Weierstrass zeta function).

In the presence of the evolving vortex system, a passive particle with position given by  $z(t)$  advects according to

$$\frac{dz^*}{dt} = \frac{1}{2\pi i} \sum_{\beta=1}^n \Gamma_\beta \phi_{\mathcal{X}}(z - z_\beta(t)) \quad (2.3)$$

with the function  $\phi_{\mathcal{X}}$  the same as above. One may think of the passive particle as a vortex with zero circulation, and so the advection problem is the analog of the Newtonian  $(N+1)$ -body problem.

The equations of motion for the plane and array case are well known. For a derivation of the equations for vortex lattices see [O] and [SA]. The function  $\phi$  is usually thought of as representing the contribution of a single vortex. It has a simple pole at the position of the vortex and thus contributes a delta function to the curl of the velocity field. Note, however, that in the lattice case the function  $\phi_{\mathcal{A}}$  is not meromorphic. This is a reflection of a property of doubly-periodic meromorphic (i.e. elliptic) functions, namely, the residues of the poles in a fundamental parallelogram must sum to zero (equivalently, by Greens' Theorem, a doubly-periodic vector field must have zero net curl in each fundamental parallelogram). Thus the concept of a single doubly-periodic vortex or of a lattice (as we have defined it) with non-zero net circulation requires additional consideration. On the other hand, if  $\sum \Gamma_\alpha = 0$ , as will be assumed below, the right hand side of (2.3) is an elliptic function of  $z$  and one may speak without contradiction of the effect of the entire lattice on a passive particle.

**§2.2 The Hamiltonian framework.** It is well known that the equations of motion for systems of point vortices can be put into the framework of classical Hamiltonian mechanics. For an  $N$ -vortex system the phase space is  $\mathbb{C}^N - \Upsilon_{\mathcal{X}}$  where  $\Upsilon_{\mathcal{X}}$  is the *collision set* defined in the various cases as

$$\begin{aligned} \Upsilon_{\mathcal{P}}(z) &= \{(z_1, \dots, z_N) \in \mathbb{C}^N : z_i = z_j \text{ for some } i \neq j\} \\ \Upsilon_{\mathcal{A}}(z) &= \{(z_1, \dots, z_N) \in \mathbb{C}^N : z_i = z_j + nL \text{ for some } i \neq j, n \in \mathbb{Z}\} \\ \Upsilon_{\mathcal{L}}(z) &= \{(z_1, \dots, z_N) \in \mathbb{C}^N : z_i = z_j + 2n\omega_1 + 2m\omega_2 \text{ for some } i \neq j, n, m \in \mathbb{Z}\}. \end{aligned}$$

The  $x$  and  $y$  positions of each vortex,  $x_\alpha$  and  $y_\alpha$ , are conjugate variables, so the dynamical system is  $2N$ -dimensional. The Hamiltonian system has  $N$  degrees of freedom, but there is no configuration space in the usual sense. Put in geometric language, the Hamiltonian is defined on a  $2N$ -dimensional symplectic manifold that is not a cotangent bundle.

In all cases the real-valued Hamiltonian takes the form

$$H_{\mathcal{X}}(z_1, \dots, z_N) = -\frac{1}{4\pi} \sum' \Gamma_\alpha \Gamma_\beta \Phi_{\mathcal{X}}(z_\alpha - z_\beta) \quad (2.4)$$

where the sum is over all  $\alpha$  and  $\beta$ , and the primed summation symbol indicates that the case  $\alpha = \beta$  is excluded. The function  $\Phi_{\mathcal{X}}$  (essentially the real part of the antiderivative of  $\phi_{\mathcal{X}}$ ) in the various cases is

$$\begin{aligned} \Phi_{\mathcal{P}}(z) &= \log(|z|) \\ \Phi_{\mathcal{A}}(z) &= \log(|\sin(\frac{\pi}{L}z)|) \\ \Phi_{\mathcal{L}}(z) &= \log(|\sigma(z)|) + \operatorname{Re}(\frac{\delta z^2}{2}) - \frac{\pi}{2\Delta} z z^* \end{aligned} \quad (2.5)$$

with  $\sigma(z)$  the Weierstrass sigma function with half periods  $\omega_1$  and  $\omega_2$ . The equations of motion (2.1) then have the form

$$\Gamma_\alpha \frac{dz_\alpha^*}{dt} = \frac{\partial H}{\partial y_\alpha} + i \frac{\partial H}{\partial x_\alpha}. \quad (2.6)$$

The presence of the factor  $\Gamma_\alpha$  on the left hand side indicates that in order to put the equations in the proper Hamiltonian form we need to change coordinates or else use a slightly nonstandard symplectic form. We choose the latter course and adopt the form

$$\sum \Gamma_\alpha dx_\alpha \wedge dy_\alpha, \quad (2.7)$$

and so the skew-symmetric matrix representing the form is

$$\Omega = \begin{pmatrix} 0 & -\Gamma \\ \Gamma & 0 \end{pmatrix}$$

with  $\Gamma = \operatorname{diag}(\Gamma_\alpha)$ . Thus if  $W = (x_1, \dots, x_N, y_1, \dots, y_N)$ , the equations of motion (2.2) become

$$\Omega \frac{dW}{dt} = \nabla H$$

with  $\nabla$  the real gradient.

It is clear from equations (2.1) that the complex quantity  $J = \sum \Gamma_\alpha z_\alpha$  is a constant of the motion. This integral is associated with the invariance of the Hamiltonian under simultaneous planar translation of all the vortices. Writing  $J = Q + iP$  with  $P$  and  $Q$  real-valued, and using the symplectic form (2.7), the Poisson bracket of  $P$  and  $Q$  is  $\{P, Q\} = (\nabla P)^T (\Omega^{-1})^T \nabla Q = \sum \Gamma_\alpha$ . Throughout most of this paper we will be assuming that  $\sum \Gamma_\alpha = 0$ , and so  $P$  and  $Q$  are in involution. The gradients of  $P$  and  $Q$  are obviously independent. Thus in the case  $N = 3$  the system (2.6) is completely integrable. The structure of the level sets is discussed in §3.5 below.

The advection equation (2.3) may also be put in Hamiltonian form. Assuming that a motion  $\{z_\beta(t)\}$  of the  $N$  vortices is given, the time-dependent real-valued Hamiltonian is

$$G_{\mathcal{X}}(z) = -\frac{1}{2\pi} \sum_{\beta=1}^N \Gamma_\beta \Phi_{\mathcal{X}}(z - z_\beta(t)). \quad (2.8)$$

In this case we use the standard symplectic form on the plane. The function  $G_{\mathcal{X}}$  is more commonly called the *stream function* of the advection problem. The right hand side of (2.8) is the velocity field of an unsteady two-dimensional fluid motion generated by the evolving collection of vortices.

One can also combine the systems (2.4) and (2.8) into a single  $(N+1)$ -degree of freedom system, but we do not pursue this point of view here.

### §3 Symmetry and reduction.

The evolution of the vortex systems is certainly independent of the choice of the origin. This is reflected in the invariance of the Hamiltonian (2.4) under simultaneous translation of all the vortices. There is a well-known process going back to Jacobi and Poincaré which uses such symmetries to reduce the effective dimension of a Hamiltonian system. This process of *reduction* proceeds by first fixing a value of the integrals arising from the symmetries and then identifying elements in the level set that correspond under the restricted symmetry. The resulting reduced system is Hamiltonian and has one less degree of freedom for every independent continuous symmetry. The mathematical theory of reduction has been much developed in recent years (see, for example, [M], Appendix 5 in [A2], or Chapter V.D in [MH]). We shall need only a small piece of the theory here. Reduction for vortices in the infinite plane is described in greater generality in [AR].

In addition to the continuous symmetries, vortex arrays and lattices have discrete symmetries that describe their periodicities. The utilisation of the discrete symmetries is rather different than continuous ones, resulting in a change of the topology of the phase space rather than a reduction of dimension.

**§3.1 Group actions.** Symmetries are usually described by invariance under a group action. If  $G$  is a group (which we write additively), an action of  $G$  on a space  $X$  is a (at least continuous) map  $G \times X \rightarrow X$ , where  $g \cdot x$  is written for the image of  $(g, x)$ . The action is required to satisfy  $0 \cdot x = x$  and  $(g_1 + g_2) \cdot x = g_1 \cdot (g_2 \cdot x)$ . The *orbit* or *trajectory* through  $x$  is the image of  $x$  under all the group elements, sometimes written  $G \cdot x = \{g \cdot x : g \in G\}$ .

Given a Hamiltonian  $H : X \rightarrow \mathbb{R}$  and an action of the group  $G$ , the Hamiltonian is said to be invariant under the group action if  $H(g \cdot x) = H(x)$  for all  $x \in X$  and  $g \in G$ . Because of this invariance the Hamiltonian will be constant on the orbits of the action. Thus if we create a new space by identifying all the points on the same orbit, we will get a new Hamiltonian function on the quotient space. This process of collapsing orbits to points is called *factoring or mod-ing* out by the group.

A group action is also generated by the collection of solutions to an autonomous ordinary differential equation,  $\dot{x} = F(x)$  with  $x \in X$  (if both  $F$  and  $X$  are sufficiently well behaved). This action of  $\mathbb{R}$  on  $X$  is usually written  $\psi : X \times \mathbb{R} \rightarrow X$  and it satisfies  $\partial\psi(x, t)/\partial t = F(\psi(x, t))$ . In Dynamical Systems this action is called a *flow*, and here we use flow exclusively in this sense. The evolution of a fluid is called a *fluid motion*. Note that if a fluid motion is steady in a region  $X$ , then the evolution of passive scalars (advection) is described by a

mathematical flow. However, if the velocity field  $F$  depends on  $t$ , the motion of the fluid is not a flow in the sense used here. One can obtain a flow on a new space  $X \times \mathbb{R}$  by defining a new variable  $\tau \in \mathbb{R}$  with  $\dot{\tau} = 1$  and letting  $\dot{x} = F(x, \tau)$ .

For Hamiltonian systems, invariance under a group action is closely related to integrals of motion: if  $H$  is invariant under an action of  $\mathbb{R}$  and this action is the same as the flow induced by another Hamiltonian  $\hat{H}$ , then  $\hat{H}$  is an integral invariant of the original Hamiltonian system. If there are  $k$  independent symmetries that commute (usually expressed as an action of  $\mathbb{R}^k$ ), then there will be  $k$  independent integrals of motion.

**§3.2 Continuous and discrete symmetries of the vortex systems.** The Hamiltonian (2.4) is invariant under simultaneous translation of all the vortices,

$$H_{\mathcal{X}}(z_1 + \tau, \dots, z_N + \tau) = H(z_1, \dots, z_N) \quad (3.1)$$

for  $\tau \in \mathbb{C}$ . This action of  $\mathbb{C}$  (or  $\mathbb{R}^2$ ) is called the *continuous symmetry*. It gives rise to the integral of motion  $J := Q + iP$  defined in §2.2.

In addition to the continuous symmetries, vortex arrays and lattices have a symmetry associated with their periodicity. For arrays,

$$H_{\mathcal{A}}(z_1 + n_1 L, \dots, z_N + n_N L) = H_{\mathcal{A}}(z_1, \dots, z_N) \quad (3.2)$$

for all collections of integers  $n_1, n_2, \dots, n_N$ . Thus the Hamiltonian is invariant under an action of  $\mathbb{Z}^N$ . In the lattice case the Hamiltonian is invariant under a  $(\mathbb{Z}^2)^N$  action,

$$H_{\mathcal{L}}(z_1 + n_1 2\omega_1 + m_1 2\omega_2, \dots, z_N + n_N 2\omega_1 + m_N 2\omega_2) = H_{\mathcal{L}}(z_1, \dots, z_N). \quad (3.3)$$

We shall call these the *discrete symmetries*.

**§3.3 Reduction and reconstruction using formulae.** From this point onward we restrict to the case of three vortices,  $N = 3$ . In addition, the sum of the circulations is assumed to be zero,  $\sum \Gamma_\beta = 0$ .

If  $Z = z_1 - z_2$ , then using the definition of  $J$  and the fact that  $\sum \Gamma_\alpha = 0$ ,

$$\begin{aligned} z_2 - z_3 &= \frac{-J + \Gamma_1 Z}{\Gamma_3} \\ z_1 - z_3 &= \frac{-J - \Gamma_2 Z}{\Gamma_3}. \end{aligned} \quad (3.4)$$

Substituting this into the result of subtracting the first two equations of (2.1) yields

$$\frac{dZ^*}{dt} = \frac{-\Gamma_3}{2\pi i} (\phi_{\mathcal{X}}(Z) + \phi_{\mathcal{X}}(\frac{-J + \Gamma_1 Z}{\Gamma_3}) + \phi_{\mathcal{X}}(\frac{J + \Gamma_2 Z}{\Gamma_3})). \quad (3.5)$$

This is a one degree of freedom system with Hamiltonian

$$K_{\mathcal{X}}(Z) = \frac{\Gamma_3}{2\pi} (\Phi_{\mathcal{X}}(Z) + \frac{\Gamma_3}{\Gamma_1} \Phi_{\mathcal{X}}(\frac{-J + \Gamma_1 Z}{\Gamma_3}) + \frac{\Gamma_3}{\Gamma_2} \Phi_{\mathcal{X}}(\frac{J + \Gamma_2 Z}{\Gamma_3})) \quad (3.6)$$

using the standard symplectic form (phase portraits in a planar and array example are shown in Figures 3.1 and 3.2, respectively). Thus the two independent integrals  $Q$  and  $P$

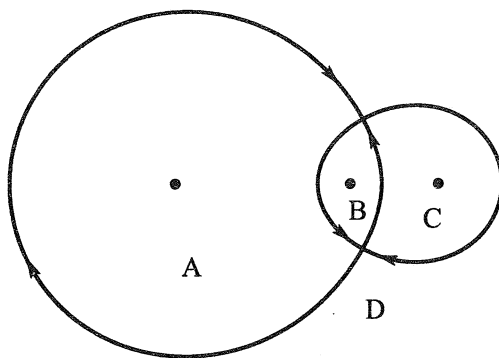


**Figure 3.1:** Phase portrait of the reduced Hamiltonian system for three vortices in the infinite plane with circulations  $1, 1/2$  and  $-3/2$ . The upper case letters label regimes discussed in §4.3.

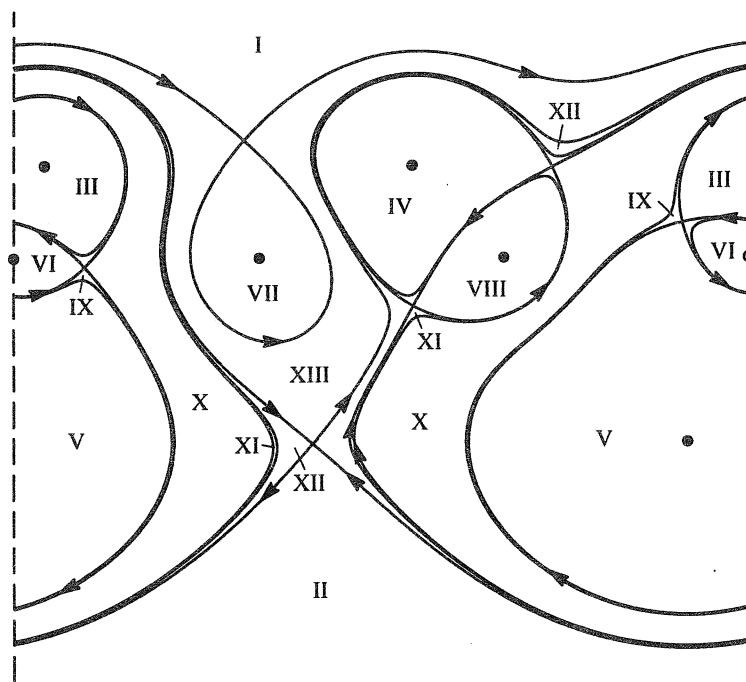


**Figure 3.2:** Phase portrait of the reduced Hamiltonian system for three vortices in a singly-periodic array with circulations  $1, 1/2$  and  $-3/2$ . The Roman numerals label regimes discussed in §4.5.

have reduced the system by two degrees of freedom, from three to one. However, the way in which the continuous symmetries have brought about the reduction is not clear. One would expect that  $K_{\mathcal{X}}$  could be obtained by substituting (3.4) into the Hamiltonian (2.4), but there is an unexplained factor of  $-\frac{\Gamma_1 \Gamma_2}{\Gamma_3}$ .

When  $\Gamma_3$  is an integer the discrete symmetries in the array case are reflected in the invariance of  $K_{\mathcal{A}}$  under translations by  $\Gamma_3 L$ . Thus we may think of the reduced system as living on a cylinder of width  $\Gamma_3 L$ . But although  $z_1$  and  $z_2$  have a width  $L$  symmetry, why should their difference have a width  $\Gamma_3 L$  symmetry? These questions are answered using the geometric framework of the next subsection.



Reconstruction refers to the process of obtaining solutions to the full equations (2.1) from the reduced one (3.5). After fixing a value of  $J$ , this may be done by “quadrature”. Explicitly, using (3.4) in the differential equation (2.1) for  $z_1$ ,

$$\frac{dz_1}{dt} = \frac{1}{2\pi i} (\Gamma_2 \phi_{\mathcal{X}}(Z(t)) + \Gamma_3 \phi_{\mathcal{X}}(\frac{-J - \Gamma_2 Z}{\Gamma_3})). \quad (3.7)$$

Thus once an initial position  $z_1(0)$  is chosen,  $z_1(t)$  may be obtained by integrating (3.7), and then  $z_2(t) = z_1(t) - Z(t)$  and (3.4) yields  $z_3(t)$ .

Note that if  $Z(t)$  is given and the initial position of the first vortex  $z_1(0)$  is changed by a translation to  $\hat{z}_1(0) = z_1(0) + \tau$  for  $\tau \in \mathbb{C}$ , then the entire motion translates by  $\tau$ , i.e. the new solution are  $\hat{z}_\alpha(t) = z_\alpha(t) + \tau$ , for  $\alpha = 1, 2, 3$ . Also note that if  $Z(t)$  is periodic with period  $P$ , (3.7) shows that the vortex positions  $z_\alpha(t)$  will, in general, not be periodic. Rather there will be a constant  $b \in \mathbb{C}$  with  $z_\alpha(t + P) = z_\alpha(t) + b$ , for all  $t$  and  $\alpha$ . The number  $b$  is an example of a dynamic phase which is also best understood in the geometric framework of the next subsection.

**§3.4 Reduction in the geometric framework.** For most of the remainder of this section we restrict to the case of singly-periodic arrays and drop the subscripts in various notations, so  $\phi = \phi_{\mathcal{A}}$ , etc. For expositional simplicity, let  $L = 1$ .

A natural starting point is the observation that the system does not change if we pick an integer  $n$  and change  $z_\alpha$  to  $z_\alpha + n$ . This means that we may treat each  $z_\alpha$  as a singly-periodic variable, i.e. an element of a cylinder  $S^1 \times \mathbb{R}$ . This is equivalent to factoring out by the  $(\mathbb{Z})^3$  symmetry and obtaining a Hamiltonian system with phase space  $(S^1 \times \mathbb{R})^3 - \Upsilon$ . Unfortunately the integral  $Q = \sum \Gamma_\alpha x_\alpha$  is not well defined as a function of the singly-periodic  $x$ -coordinates. Put another way, the continuous symmetry of the  $\mathbb{R}^2$ -action is still present in the factored system, but it is no longer Hamiltonian in character; the one-parameter subgroup that translates in the  $y$ -direction is not a Hamiltonian flow *on the product of cylinders*. Thus we proceed by first reducing the system by the continuous symmetries and then using the discrete symmetries.

Fix a value of the integrals, say  $J_0 = Q_0 + iP_0$ , and let  $A_0$  be the integral manifold (level set)

$$A_0 = \{(z_1, z_2, z_3) : \sum \Gamma_\alpha z_\alpha = J_0\}.$$

It is convenient to use coordinates  $(Z, Y)$  for  $A_0$  with  $Z = a_1 - a_2$  and  $Y = a_1$  for  $\mathbf{a} = (a_1, a_2, a_3) \in A_0$ . Since  $\sum \Gamma_\alpha (a_\alpha + \tau) = \sum \Gamma_\alpha a_\alpha$ , the set  $A_0$  is invariant under the action of  $\mathbb{R}^2$  as well as under the Hamiltonian flow. In coordinates,  $\tau \in \mathbb{R}^2$  acts as  $(Z, Y + \tau)$ . We now mod out by the  $\mathbb{R}^2$  action restricted to  $A_0$ , i.e. we consider  $\mathbf{a}$  and  $\mathbf{a} + \tau(1, 1, 1)$  to be the same point; in coordinates this just amounts to identifying  $Y$  with  $Y + \tau$  for all  $\tau \in \mathbb{C}$ . The reduced space, denoted  $R$ , is thus a copy of the complex plane coordinatized by  $Z$ . The Meyer-Marsden-Weinstein Theorem (see [M]) assures us that  $R$  has a unique symplectic form that pulls back under the projection  $A_0 \rightarrow R$  to the restriction of of the form  $\Omega$  on  $A_0$ . To compute this form on  $R$ , note that restricted to  $A_0$ ,  $\sum \Gamma_\alpha dx_\alpha = 0 = \sum \Gamma_\alpha dy_\alpha$ . Then using  $\sum \Gamma_\alpha = 0$ ,

$$\sum \Gamma_\alpha dx_\alpha \wedge dy_\alpha = \frac{-\Gamma_1 \Gamma_2}{\Gamma_3} (dx_1 - dx_2) \wedge (dy_1 - dy_2) = \frac{-\Gamma_1 \Gamma_2}{\Gamma_3} dZ^1 \wedge dZ^2$$

where  $Z = Z^1 + iZ^2$ . Thus the proper symplectic form on  $R$  is  $-\frac{\Gamma_1\Gamma_2}{\Gamma_3}$  times the standard one. The flow restricted to  $A_0$  projects to a Hamiltonian flow on  $R$ , and the Hamiltonian is obtained by substituting (3.4) into the Hamiltonian (2.4) of the full system. As noted above, this substitution yields (3.6) without a factor  $-\frac{\Gamma_1\Gamma_2}{\Gamma_3}$ , a factor now explained by the proper symplectic structure on  $R$ .

The next step is to connect the Hamiltonian flow on  $R$  with the full flow on  $A_0$  (this is the reconstruction step). The flow on  $A_0$  may be expressed as

$$(Z(t; Z_0), Y(t; Y_0, Z_0)) \quad (3.8)$$

with the symbols after the semicolon representing the initial conditions. Note that the evolution of the  $Z$  coordinate just depends on the  $Z$  initial condition and not on  $Y$ . The invariance of the Hamiltonian under the  $\mathbb{R}^2$ -action is expressed by

$$(Z(t; Z_0), Y(t; Y_0 + \tau, Z_0)) = (Z(t; Z_0), Y(t; Y_0, Z_0)) + \tau. \quad (3.9)$$

In more concrete terms, the variable  $Z = z_1 - z_2$  in conjunction with the fixed value of  $J$  determines the shape and orientation of the triangle determined by the vortices. The variable  $Y = z_1$  gives its position. Translating this position by  $\tau$  has only the effect of translating the entire evolution by  $\tau$ .

Since the Hamiltonian system on  $R$  has just one degree of freedom, the generic bounded orbit is periodic. Thus after some period  $P$ , the shape and orientation of the triangle of vortices will be reestablished, but in general, the entire configuration could have translated by some amount. This amount is the *dynamic phase* and is equal to

$$b(Z_0) := Y(P; Y_0, Z_0) - Y(0; Y_0, Z_0) \quad (3.10)$$

with  $Z_0$  an element of the chosen periodic orbit. By virtue of (3.9) this expression is independent of  $Y_0$ . In geometric language this phase represents the return map (holonomy) in the fiber of the bundle  $A_0 \rightarrow R$  as one goes around the periodic orbit loop in  $R$ . The numerical value of the phase may be obtained from  $Z(t)$  by integrating (3.7).

Thus far we have focused on the role of the continuous symmetries in reducing the number of degrees of freedom of the vortex systems. The use of the discrete symmetries in the array and lattice systems will be called *factoring* to distinguish it from reduction. For expositional simplicity we now assume that  $\Gamma_1 = 1$  and will freely use this numerical value as well as the symbol in various formulas. This results in no loss of generality because equations (2.1) show that rescaling all circulations by the same amount only changes the speed (and perhaps the direction) of the vortices, but does not change their trajectories.

The main observation required in using the discrete symmetries in the reduction process is that additional symmetries can only be used if they preserve the level sets  $A_0$ , or equivalently, the value of the integral  $J$ . If  $(a_1, a_2, a_3)$  is in  $A_0$  there is no guarantee that  $(a_1 + n_1, a_2 + n_2, a_3 + n_3)$  is in  $A_0$  for arbitrary  $(n_1, n_2, n_3)$ . However, it is easy to find conditions that insure this, namely,  $\sum \Gamma_\alpha n_i = 0$ . The set of all such  $(n_1, n_2, n_3)$  is a subgroup of  $\mathbb{Z}^3$  which we denote  $\mathbf{K}$ . This subgroup always contains all multiples of  $(1, 1, 1)$  and is larger exactly when  $\Gamma_3$  is rational. Since translation by integer multiples of  $(1, 1, 1)$  is contained in the continuous action, the discrete symmetries only come into play when  $\Gamma_3$  is rational.

An element  $(k_1, k_2, k_3) \in \mathbf{K}$  acts on  $A_0$  as  $(a_1 + k_1, a_2 + k_2, a_3 + k_3)$ , and so it acts in coordinates as

$$(Z + (k_1 - k_2), Y + k_1). \quad (3.10)$$

But note that  $(k_1 - k_2) = \Gamma_3(k_2 - k_3)$ , and thus the action of  $\mathbf{K}$  on  $R$  just adds  $\Gamma_3$  times an integer to the coordinate  $Z$ . When  $\Gamma_3$  is irrational,  $k_1 = k_2 = k_3$ , and  $\mathbf{K}$  does not act on the  $Z$  component. When  $\Gamma_3 = p/q$  is rational (in lowest terms),  $k_1 - k_2$  is actually  $p$  times an integer because the  $k_i$  are integers. Thus the induced symmetry on  $R$  is translation by  $p$ . Algebraically speaking, the map  $(k_1, k_2, k_3) \mapsto (k_1 - k_2, k_1)$  is an isomorphism from  $\mathbf{K}$  to  $p\mathbb{Z} \oplus \mathbb{Z}$ . In this new form  $\mathbf{K}$  acts on  $R$  with just its first factor. Thus the action of  $\mathbf{K}$  on  $R$  induces a mod  $p$  symmetry on the plane  $R$ . The Hamiltonian on  $R$  thus has a mod  $p$  symmetry and so the final factored system has a cylinder of width  $p$  as its phase space. Figure 3.2 shows the orbits of the reduced system for a vortex array with  $\Gamma_1 = 1, \Gamma_2 = 1/2$  and  $\Gamma_3 = -3/2$ . The left and right edges of the box can evidently be identified to get a width 3 cylinder.

In the case of lattices, there is a discrete action on both the real and imaginary parts of  $z_\alpha$ . Thus if  $\Gamma_3 = p/q$ , the factored system may be considered a torus with width and length  $p$ , i.e. a Hamiltonian on  $\mathbb{R}^2/p\mathbb{Z}^2$ .

**§3.5 Integral manifolds and dynamics.** As noted in §2.2, in the case  $N = 3$  the vortex systems are completely integrable as Hamiltonian systems. Orbits of the phase flow are constrained to simultaneous level sets of  $H, Q$  and  $P$ . If the phase space was compact, these integral manifolds would be generically tori. The systems here do not have compact phase spaces, but the reduction and subsequent reconstruction make the structure of the integral manifolds clear.

In the reduced space  $R$  the generic, bounded level set of  $K_\chi$  is a topological circle (dynamically a periodic orbit). If we fix one such circle  $C \subset R$ , then an integral manifold  $\Lambda$  of the full system corresponding to fixing values of  $H, Q$  and  $P$  is the preimage of  $C$  under the projection  $A_0 \rightarrow R$ . Thus the generic  $\Lambda$  is homeomorphic to  $C \times \mathbb{R}^2$  with the  $\mathbb{R}^2$  factor coordinatized by  $Y$ . The flow on  $\Lambda$  factors as in (3.8). The simplest way to understand this flow is to examine the return map of orbits to the  $\mathbb{R}^2$  factor as one travels around  $C$ . By (3.9) and (3.10) this return map is translation by  $b(Z_0)$  for any  $Z_0 \in C$ .

In the array case when  $\Gamma_3$  is rational we have used the action of the discrete symmetry in the first coordinate of (3.10) to factor  $R$ . One also sees from (3.10) that the action of the discrete symmetry on the  $Y$ -component is addition of an integer. This action can be used to factor the second component of  $\Lambda$  to obtain an integral manifold homeomorphic to  $C \times (S^1 \times \mathbb{R})$  with the return map to the cylinder factor now addition of  $b(Z_0)$  (reduced mod 1 in the first coordinate). The lattice case is similar, but the discrete symmetries yield integral manifolds  $C \times (S^1 \times S^1)$ . Depending on the value of  $b(Z_0)$ , the flow on these tori can have 1, 2 or 3 independent frequencies.

**§3.6 Irrational circulation ratios and quasi-periodicity.** We now use the continuous and discrete symmetries from a slightly different point of view with the goal of illuminating the case of irrational circulation ratios and the resulting quasi-periodicity in the reduced Hamiltonian system. We factor by the action of the discrete and then the continuous symmetry. The level sets of  $J$  descend to invariant subsets, but they are no longer level sets of a real-valued function. The focus here is on the lattice case and we comment on the array case at the end. The nomenclature *n-torus* refers to the topological space  $\mathbb{T}^n := (S^1)^n$ , i.e. the  $n$ -dimensional manifold that is periodic in all  $n$  directions.

Recall that the phase space of the Hamiltonian system describing the vortex motions is  $\mathbb{C}^3 - \Upsilon_{\mathcal{L}}$ , which is denoted here as  $\mathcal{Y}$ . The discrete action of  $\mathbb{Z}^3$  on  $\mathcal{Y}$  factors the phase

space to  $(S^1 \times S^1)^3 - \Upsilon'$  which we give coordinates  $(\nu_1, \nu_2, \nu_3)$ , where  $\Upsilon'$  is the factored collision set. (Note that each  $S^1 \times S^1$  is a Lie Group; one does arithmetic by reducing mod 1 in both factors.) The continuous symmetry of  $\mathbb{R}^2$  acts by simultaneous addition on all 2-tori, so  $\tau \in \mathbb{R}^2$  acts as  $(\nu_1 + \tau, \nu_2 + \tau, \nu_3 + \tau)$ . Identifying points under this action yields a quotient space  $\hat{\mathcal{Y}} = (S^1 \times S^1)^2 - \hat{\Upsilon}$  with coordinates  $(\nu_1 - \nu_2, \nu_2 - \nu_3) := (U, V)$  and  $\hat{\Upsilon} = \{U = 0\} \cup \{V = 0\} \cup \{U = V\}$ . The Hamiltonian (2.4) on  $\mathcal{Y}$  descends to

$$\hat{H}(U, V) = -\frac{1}{2\pi}(\Gamma_1\Gamma_2\phi(U) + \Gamma_2\Gamma_3\phi(V) + \Gamma_1\Gamma_3\phi(U + V)). \quad (3.11)$$

If  $\Gamma_3$  is an integer, the integral  $J$  may be expressed in these coordinates as  $\hat{J}(U, V) = U - \Gamma_3 V$  (recall that  $\Gamma_1 = 1$ ) with  $\hat{J}$  having values in a 2-torus with width  $\Gamma_3$  in both directions. If  $\Gamma_3$  is irrational, no such adaptation may be made. But in any case, since a level set  $A_0$  of  $J$  is invariant under the Hamiltonian flow, the projection  $\hat{A}_0$  to  $\hat{\mathcal{Y}}$  is invariant under the Hamiltonian flow induced by  $\hat{H}$ .

We now treat  $\hat{\mathcal{Y}}$  as a subset of the 4-torus,  $\mathbb{T}^4$ . If  $\Gamma_3$  is irrational, the level set  $\hat{A}_0$  is an immersed two-plane that winds densely in the four torus. The Hamiltonian  $\hat{H}$  on  $\mathbb{T}^4$  restricted to  $A_0$  is the same as the reduced Hamiltonian on  $R$  given in (3.6). Thus this Hamiltonian induces a quasiperiodic system on  $R$  in the sense of [A1]. The function  $\hat{H}$  has singularities when  $U = 0$ ,  $V = 0$  or  $U = -V$ , each of which represents a plane in  $\mathbb{T}^4$ . The intersection of these planes with the densely wrapped plane  $A_0$  yield the poles of the reduced Hamiltonian  $K_{\mathcal{L}}$ . Thus the collection of poles are a quasi-crystal, at least according to one definition of that term ([J], [A1]).

Since (the complexification of)  $\hat{H}$  has simple poles, the poles of the restricted Hamiltonian on any  $\hat{A}_0$  will also be simple. Thus it is plausible that the flow on  $R$  (or  $\hat{A}_0$ ) can be treated as advection in the presence of fixed vortices with circulations given by the residues of the poles. The precise sense in which this is true is given in [SA] and [AS2]. Further, it is shown in [AS2], that this collection of fixed vortices is dynamically fixed as well, i.e. if these vortices are allowed to interact with each other, they will still be stationary. In other language, the collection of poles of the reduced Hamiltonian on  $R$  forms an equilibrium configuration of the planar  $N$ -vortex problem.

This viewpoint can also be used to illuminate what happens as the various parameters in the system are varied. For example, once the  $\Gamma_\alpha$  are fixed, changing  $J_0$  just translates  $\hat{A}_0$  and does not alter its “slope”. Thus there will be no qualitative changes in the pattern of the poles of  $\hat{A}_0$  except for the exceptional values of  $J_0$  which cause it to hit the triple intersection points  $U = V = 0$  (the integer lattice). On the other hand, if the  $\Gamma_\alpha$ ’s are varied, the background flow changes as does the slope of the  $\hat{A}_0$ . However, the singularity planes remain the same, so it is easy to track the singularities on  $\hat{A}_0$ . In particular, if there is a sequence of rational  $\Gamma_3^{(n)} = \frac{p_n}{q_n}$  with  $\frac{p_n}{q_n} \rightarrow \Gamma_3^0$  with  $\Gamma_3^0$  irrational, then the periodic systems will converge to the quasiperiodic one after the appropriate rescalings.

A similar analysis can be applied to the array case, but now if  $\Gamma_3$  is irrational the quasiperiodicity of the reduced Hamiltonian  $K_{\mathcal{A}}$  will only be in the real direction.

#### §4 Regimes and braids.

Braids are the standard mathematical tool for describing the topology of periodic motions of collections of points in the plane. In this section braids are used to describe the motions

of point vortices. While a braid may be used to describe the periodic motion of any number of vortices, the analysis is particularly simple in the case of three vortices. As we have seen in §3 when the total circulation is zero, the generic motion in the reduced plane is periodic. Thus the corresponding motion of the vortices is periodic after adjusting for the dynamic phase, and so may be described by a braid.

**§4.1 Braids and braid types.** This subsection gives a brief introduction to braids from a point of view useful for the applications that follow. For broader perspective and additional information see [Bm1] or [BL]. Braids are used to describe the motions of the bodies in the planar  $N$ -body problem by Montgomery [Mt].

A *physical or geometric braid* is a collection of noncrossing paths in  $\mathbb{R}^3$  that start at some finite collection of points  $E$  on the plane where the third coordinate is zero and end at the same set of points (perhaps permuted) on the plane where the third coordinate is one. More formally, a physical braid on  $n$  strands is a collection of maps  $\mathbf{b} = \{b_1, \dots, b_n\}$ , with each  $b_i : [0, 1] \rightarrow \mathbb{R}^3$  and (1) each  $b_i$  has the form  $b_i(t) = (a_i(t), t)$  with each  $a_i$  continuous, (2) for all  $t \in [0, 1]$ ,  $b_i(t) \neq b_j(t)$  for  $i \neq j$ , and (3) the set of initial points is identical to the set of final points  $E = \{a_1(0), a_2(0), \dots, a_n(0)\} = \{a_1(1), a_2(1), \dots, a_n(1)\}$ . The initial and final points of the braid are collectively called the *endpoints*. The collection of trajectories  $\{a_i(t)\}$  is called the *plane motion of the braid*.

A *mathematical braid* on  $n$  strands is an element of the braid group  $B_n$ . This group is defined as possessing the  $n$  generators  $\sigma_1, \sigma_2, \dots, \sigma_n$  with inverses denoted  $\bar{\sigma}_1, \bar{\sigma}_2, \dots, \bar{\sigma}_n$  and the relations  $\sigma_i \sigma_j = \sigma_j \sigma_i$  for  $|i - j| > 1$  and  $\sigma_i \sigma_{i+1} \sigma_i = \sigma_{i+1} \sigma_i \sigma_{i+1}$  for all  $i$  ([Bm1]). A *braid word* refers to a sequence of “letters”, with each letter being one of the  $\sigma_i$  or their inverses. The inverse of a generator is indicated by an overbar,  $\bar{\sigma}_i$ . Two braid words are said to be equivalent if they represent the same element in the braid group, i.e. one can be transformed into the other using the relations in the group. The identity element in  $B_n$  is denoted  $e$ .

The assignment of a mathematical braid to a physical one requires a plane onto which projections are made. The convention here is to let this plane in  $\mathbb{R}^3$  be  $y = k$  for some large negative  $k$ . If we treat the  $xy$  plane as the complex numbers, projection of  $\mathbf{b}$  onto the chosen plane yields a family of curves  $(\text{Re}(a_i(t)), t)$ . An *ij-crossing* is a point where  $\text{Re}(a_i(t)) = \text{Re}(a_j(t))$  for some  $t$  and  $i \neq j$ . The braid word will record which strand is in front at each crossing or, more precisely, which of the  $b_i(t)$  is closest to the projection plane.

The braid word corresponding to  $\mathbf{b}$  is read off from the picture of the projection. Assume for the moment that all crossings are transverse and take place at distinct times. Starting from the bottom, examine the first crossing. If the  $i^{\text{th}}$  strand from the left crosses behind the  $(i+1)^{\text{st}}$ , write down the letter  $\sigma_i$ . If it crosses in front, write  $\bar{\sigma}_i$ . Now continue upward in the projection checking each crossing and writing a braid letter. Note that the  $i^{\text{th}}$  strand at each step refers to the  $i^{\text{th}}$  strand *from the left* at that level. The physical strand that is  $i^{\text{th}}$  at one level may become  $(i+1)^{\text{st}}$  or  $(i-1)^{\text{st}}$  at the next level. It is also worth noting that contrary to the conventions of [Bm1], the convention here is that letters further to the right in a braid word encode crossings that are *higher* up the braid. We adopt this somewhat nonstandard convention because our physical braids arise from time-parameterised trajectories in the plane, and it is more natural to visualise these in  $\mathbb{R}^3$  with time going upwards.

It is natural to ask how much the mathematical braid tells us about the physical braid. In particular, which physical braids get assigned the same mathematical one? Say that two

physical braids  $\mathbf{b}$  and  $\mathbf{b}'$  with the same endpoints are *equivalent* if one can be obtained from the other by a deformation that fixes the endpoints and does not cut the strands, i.e. there is a continuous family of physical braids  $\mathbf{b}^s$  for  $s \in [0, 1]$  with  $\mathbf{b}^0 = \mathbf{b}$  and  $\mathbf{b}^1 = \mathbf{b}'$ . The relations in the braid group are chosen precisely so that two physical braids are equivalent exactly when they are assigned equivalent braid words, i.e. the same mathematical braid. A theorem of Artin's ([Bm1]) says that any equivalence between physical braids can be described in terms of just the two kinds of deformations described by the relations in the braid group.

Because equivalent physical braids are assigned equivalent braid words we can eliminate the assumption we had to make in order to assign a mathematical braid to a physical one. If  $\mathbf{b}$  does not have transverse and time-distinct crossings, deform it to another braid  $\mathbf{b}'$  that does and compute a mathematical braid for  $\mathbf{b}'$ . Since any other “good” deformation will be assigned a braid word equivalent to that of  $\mathbf{b}'$ , this braid word may be used unambiguously for  $\mathbf{b}$ .

Thus far we have restricted attention to equivalence of physical braids with the same endpoints. Since the braids here arise from vortex motions with a variety of initial positions we need to extend the notion of equivalence. Informally two braids with perhaps different endpoints are equivalent if one can be transformed into the other via a plane transformation applied on each horizontal plane followed by a deformation with fixed endpoints. More formally, two physical  $n$ -braids  $\mathbf{b}$  and  $\mathbf{b}'$  are *equivalent* if there is a homeomorphism  $h : \mathbb{R}^2 \rightarrow \mathbb{R}^2$  with  $h(a_i(0)) = a'_i(0)$  for all  $i$  and the physical braid  $\{(h(a_i(t)), t)\}$  is equivalent with fixed endpoints to  $\mathbf{b}'$ . A simple argument shows that physical braids that are equivalent in this sense are assigned conjugate elements of the braid group, i.e. the words satisfy  $w' = gw g^{-1}$ , with  $g$  an element of the braid group that represents the homeomorphism  $h$ . Note that changing the projection plane may be accomplished by a rotation in the plane, and so the mathematical braid obtained using the new projection plane will be conjugate to the original.

Since the goal here is to use braids to analyse the topology of vortex motions, topologically equivalent physical braids and physical braids viewed by different observers must be assigned the same mathematical object. The remarks of the last paragraph make it clear that this object cannot be just a mathematical braid, but rather must be a conjugacy class in the braid group, i.e. the collection of all elements conjugate to a given one (and thus conjugate to each other). These conjugacy classes were called *braid types* in a related context and that terminology is adopted here (cf. [Bd]). For simplicity of exposition in the sequel we will often speak informally of the braid associated to a physical braid, but a more careful terminology would be braid type.

**§4.2 Three vortices in the plane.** In assigning braids to the motion of three point vortices in the infinite plane we continue to focus on the case of zero net circulation,  $\sum \Gamma_\alpha = 0$ . As in §3, we fix a value of the integral  $J_0 = Q_0 + iP_0$ , perform the reduction, and obtain the Hamiltonian (3.6) on a copy of the plane  $R$  with complex coordinate  $Z$ .

Pick an initial condition  $Z_0$  in  $R$  which is contained in a periodic orbit  $Z(t) := Z(t; Z_0)$  with period  $P$ . Using (3.4), the motion  $Z(t)$  determines the evolution of the differences in the positions of the three vortices. Thus  $Z(t)$  can be used to compute the motion in the

frame of one of the vortices. In the  $z_2$ -frame this motion is described by

$$\begin{aligned} Z_1(t) &:= z_1(t) - z_2(t) = Z(t) \\ Z_2(t) &:= z_2(t) - z_2(t) \equiv 0 \\ Z_3(t) &:= z_3(t) - z_2(t) = \frac{J_0 - \Gamma_1 Z(t)}{\Gamma_3}. \end{aligned} \tag{4.1}$$

Thus all the  $Z_\alpha$ 's are periodic with period  $P$ . Note that  $z_\alpha \neq z_\beta$  for  $\alpha \neq \beta$  (i.e. the absence of collisions between vortices) is equivalent to  $Z_\alpha \neq Z_\beta$  for  $\alpha \neq \beta$ . Again using (3.4), this happens as long as  $Z(t)$  avoids the points  $p_1 := J_0/\Gamma_1, p_2 := -J_0/\Gamma_2$ , and  $p_3 := 0$ . The points  $p_\alpha$  are the *poles* of the Hamiltonian  $K_P$  from (3.6).

The vortex motions generate a physical braid by treating the vertical direction as time and defining

$$\hat{Z}_\alpha = (Z_\alpha(t), t), \tag{4.2}$$

for  $\alpha = 1, 2, 3$ . Each path  $\hat{Z}_\alpha$  then connects a point on the plane  $t = 0$  to the same point on the plane  $t = P$ , and further, since  $Z(t)$  does not pass through any of the poles, the paths do not intersect. Thus the paths yield a physical braid on three strands, which may be assigned an element of  $B_3$  as in the previous subsection.

This assignment is most easily accomplished by taking a more topological point of view. If we define  $R^\circ = R - \{p_1, p_2, p_3\}$ , then the periodic orbit  $Z(t)$  in  $R$  represents a closed curve (or loop) in  $R^\circ$ . The procedure used to construct a physical braid from  $Z(t)$  can equally well be used to assign one to any loop in  $R^\circ$ . If  $\gamma$  is a loop in  $R^\circ$ , i.e.  $\gamma : [0, 1] \rightarrow R^\circ$  with  $\gamma(0) = \gamma(1)$ , let  $Z_1, Z_2, Z_3$  represent the three paths given by (4.1) using  $Z(t) = \gamma(t)$ . The physical braid corresponding to  $\gamma$  is then generated by (4.2).

The computation of the mathematical braid corresponding to this physical braid just requires knowledge of the crossing of its strands. Since we are viewing from the negative imaginary axis, the positions of the  $Z_\alpha$  from left to right are determined by their real parts. Strands cross exactly when this order changes. This can only happen when  $\text{Re}(Z_\alpha(t)) = \text{Re}(Z_{\alpha'}(t))$ , or equivalently, when  $\text{Re}(Z(t)) = \text{Re}(p_\beta)$  where  $\beta$  is the index different from  $\alpha$  and  $\alpha'$ . Thus the vertical lines through the poles divide  $R^\circ$  into vertical strips in which the order of the  $Z_\alpha$  from left to right is constant. These vertical lines will be called *crossing lines*.

To specify the generator corresponding to the crossing of one of these lines it is also necessary to know which strand is in front. This information is determined by the sign of  $\text{Im}(Z(t_c)) - \text{Im}(p_\beta)$  when  $Z(t_c)$  lies on the crossing line  $\text{Re}(Z) = \text{Re}(p_\beta)$ . This sign can only change on a crossing line when  $\text{Im}(Z(t_c)) - \text{Im}(p_\beta) = 0$ , i.e. at the pole. Thus all the crossings on the same side of the pole correspond to the same strand being in front. We will call a component of a crossing line minus its pole a *generator arc*. The final piece of information needed to specify the generator describing a crossing is the direction that  $\gamma$  traverses the generator arc. In summary then, any two crossings of a generator arc in the same direction contribute the same generator to the braid. Thus to compute braids of loops or actual vortex motions it suffices to compute the generators corresponding to each generator arc. A sample computation is given in the next subsection.

There are two issues that need to be clarified before moving on to the example. First, unlike a mathematical loop there is no distinguished starting point for a periodic motion of the vortices. However, changing the initial point on  $Z(t)$  will only cyclically permute the generators in the braid word representing the motion. This corresponds to conjugating the

word in the braid group and this ambiguity has already been resolved using the braid type. The second issue is that the usual generators of the braid group  $B_3$  only keep track of which adjacent strands are crossing and not the numbering of the strands. Thus in assigning a braid generator to a crossing we have lost track of which vortex has crossed which; our braid word is only encoding the topological type of the interaction, and not whether, say, vortices 2 and 3 are the pair that are circling each other. However this information can be recovered easily by knowing the relative positions of the vortices at the starting point of the braid and following the strands.

**§4.3 A planar example.** Figure 4.1 shows the crossing lines for the planar case of Figure 3.1. The pair of numbers at the top of the crossing line indicate which pair of vortices are crossing. Each generator arc has a number  $j$  and an arrow; crossing the arc in the direction of the arrow contributes the positive generator  $\sigma_j$  to the braid word. Crossing in the opposite direction contributes the inverse of this generator  $\bar{\sigma}_j$ . The braid word corresponding to a loop  $\gamma(t)$  can be computed by writing in order the generators corresponding to  $\gamma(t)$ 's sequential crossings of generator arcs.

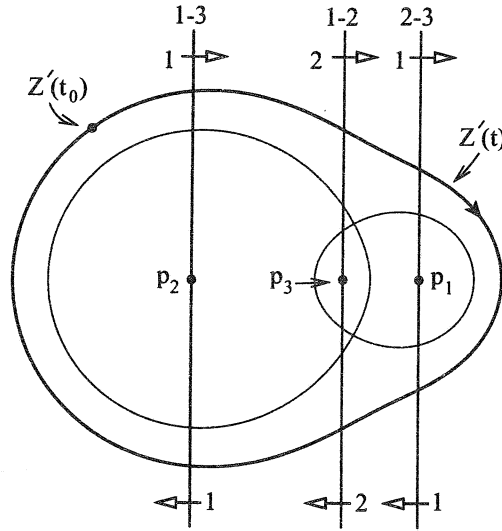


**Figure 4.1:** The crossing lines and generator arcs for the system shown in Figure 3.1.

As an example, let us compute the braid word corresponding to periodic orbit  $Z'(t)$  indicated in the region labelled D in Figure 4.1. Begin tracking the motion at the starting point labelled  $Z'(t_0)$  in the upper left hand corner. At this point the vortices from left to right are 1, 3, 2. The first generator arc crossed is above the pole  $p_2$ , it contributes a  $\sigma_1$  to the braid word. Moving across horizontally, the next generator arc contributes a  $\sigma_2$ , and so on. When we return to the initial point the entire braid word  $\sigma_1 \sigma_2 \sigma_1 \sigma_1 \sigma_2 \sigma_1$  has been read off. This braid is shown in Figure 4.2c, with the strands labelled below. By examining the braid we see that this motion corresponds to the vortices rotating clockwise around each other. Examining the braid one can see that the motion is topologically the same as all the vortices rotating once around a circle clockwise. This becomes especially clear after using the braid relation and rewriting the braid as  $(\sigma_1 \sigma_2)^3$ .

Figure 4.2a shows the planar trajectories of three vortices corresponding to the periodic



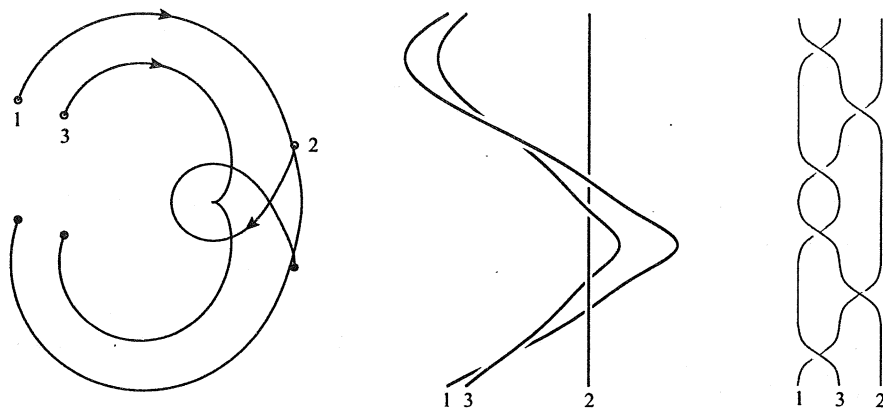


**Figure 4.2:** Vortex motions from regime D of Figure 3.1. (a) Trajectories of the three vortices in the plane. (b) Physical braid of this motion in the frame of the second vortex. (c) Mathematical braid of the motion.

orbit  $Z'(t)$ . Recall from §3.2 that there are many vortex motions corresponding to a given periodic orbit in  $R$ , but all these motions differ by a uniform translation, so it suffices to pick an initial position of one of the vortices, say  $z_2(0) = 0$ . Figure 4.2b shows the physical braid corresponding to the vortex motion in the frame of the second vortex as given by (4.1) and (4.2).

The other regions A, B, and C each contain a pole. The braid describing each of these regimes is the square of a generator and corresponds to a pair of vortices rotating about each other once per period. There is no linking with the third vortex. The pair of vortices that are involved in the rotation depends on the pole in question, and the direction of the rotation (i.e. whether the braid is  $\sigma_i^2$  or  $\bar{\sigma}_i^2$ ) depends on the signs of the circulations of the interacting vortices.

Recall that a *separatrix* is an orbit connecting two saddle points. Define a *regime* as a connected component of  $R - \{\text{poles and separatrices}\}$ . It is clear from Figure 4.1 that every periodic orbit in the same regime yields the same sequence of crossings of generator arcs, and thus the same braid word. Therefore all the motions within a regime have the same topological type of motion. More generally, any pair of loops that can be continuously deformed into each other (i.e. are homotopic) in  $R^o$  will be assigned the same braid; homotopic loops may cross different generator arcs, but any extra crossings will consist of a collection of crossings and then reverse crossings of the same generator arcs. From another point of view, deforming the loop corresponds to deforming the physical braid. The corresponding mathematical braid will only change when a pair of strands go through each other. This can only happen when the loop passes through a pole, which is not allowed as all our loop deformations are in the complement of the poles.

This situation is somewhat analogous to the residue theorem in which a deformation of a closed path in the complement of the poles does not change the value of the integral. However, the situation here is more restrictive; *homologous* loops yield the same integral but only *homotopic* loops give the same braid. In algebraic language, after fixing a basepoint for loops, the process described here gives a homomorphism from the fundamental group of the punctured plane,  $\pi_1(R^o)$ , to the braid group on three strands,  $B_3$ .

Although all periodic orbits in the same regime have the same braid, it is important to

note that the period  $P$  and dynamic phase  $b$  of the periodic orbits in a single regime can vary greatly. The period will go to zero near a pole and approach infinity as orbits near a separatrix. Thus the time scale of the actual vortex motions in the same regimes can be very different. In addition, variations in the dynamic phase can make a significant difference in the motion as observed in the lab frame.

**§4.4 Three-vortex arrays.** This subsection develops the tools needed to assign a braid to the periodic motion of three vortices in a singly-periodic array. We continue to restrict to the case of zero net circulation  $\sum \Gamma_\alpha = 0$ , fix a value of the integral  $J_0 = Q_0 + iP_0$ , and perform the reduction as in §3. The result is a Hamiltonian system given by (3.6) on a copy of the plane  $R$  with complex coordinate  $Z$ . If  $\Gamma_3$  is the rational  $p/q$  (in lowest terms), then the system on  $R$  has a mod  $p$  symmetry in the real part.

By treating each vortex position  $z_\alpha$  as a singly-periodic variable, the vortex motion can be viewed as taking place on a cylinder  $\mathbf{S}^1 \times \mathbb{R}$  (the circle  $\mathbf{S}^1$  here has perimeter one since we continue to restrict to the case  $L = 1$ ). Equivalently, in the language of §3, we factor out all the motions by the discrete symmetry. Again we eliminate the dynamic phase by passing to the frame of the second vortex, thus making the motion periodic. Accordingly, let

$$\begin{aligned} c_1(t) &:= z_1(t) - z_2(t) = Z(t) \\ c_2(t) &:= z_2(t) - z_2(t) \equiv 0 \\ c_3(t) &:= z_3(t) - z_2(t) = \frac{J_0 - \Gamma_1 Z(t)}{\Gamma_3}, \end{aligned} \tag{4.3}$$

in which properly speaking the subtraction is done in the Lie group  $\mathbf{S}^1 \times \mathbb{R}$ . The triple  $(c_1(t), c_2(t), c_3(t))$  is called the *cylinder motion* of the vortices.

A braid describes the motion of a set of points in the plane. To translate the cylinder motion to the plane, recall that the cylinder is topologically equivalent to the punctured complex plane  $\mathbb{C} - \{0\}$ . This topological equivalence is realized by the conformal map  $T(z) = \exp(2\pi iz)$ . Under this conformal map a path around the cylinder transforms to a path around the origin in the complex plane. To capture this type of motion in the braid description, we add the constant path at 0 as the last coordinate of the motion in the plane. Thus the *plane motion* of the vortices is given by

$$\begin{aligned} s_1(t) &:= T(c_1(t)) = \exp(2\pi i Z(t)) \\ s_2(t) &:= T(c_2(t)) \equiv 1 \\ s_3(t) &:= T(c_3(t)) = \exp(2\pi i \frac{J_0 - \Gamma_1 Z(t)}{\Gamma_3}) \\ s_4(t) &\equiv 0. \end{aligned} \tag{4.4}$$

Using the same technique as in the previous subsection we associate a braid (now on 4 strands) to the plane motion of a three-vortex array. Again we visualise the plane motion in three dimensions using (4.2) with time going upward and view the resulting strands from the negative imaginary axis. The *crossing curves* in  $R$  describe the positions of an orbit  $Z(t)$  at which  $s_\alpha$  and  $s_\beta$  cross; this happens when their real parts are equal. To express this in equation form, define four functions on  $R$  by  $\psi_1(Z) = T(Z)$ ,  $\psi_2(Z) = 1$ ,  $\psi_3(Z) = T((J_0 - \Gamma_1 Z)/\Gamma_3)$ , and  $\psi_4(Z) = 0$ . Then  $s_\alpha(t) = \psi_\alpha(Z(t)) = T(c_\alpha(t))$ , and the  $(\alpha, \beta)$

crossing lines are defined by the equation  $\text{Re}(\psi_\alpha(Z)) = \text{Re}(\psi_\beta(Z))$ . In contrast to the planar case, these equations no longer yield just straight lines and thus the change in terminology to crossing *curves*.

The strand which is in front at a crossing is determined by the sign of  $\text{Im}(s_\alpha(t_c)) - \text{Im}(s_\beta(t_c))$  when  $\gamma(t_c)$  is on the corresponding crossing curve. This sign changes on the crossing curve exactly when  $s_\alpha = s_\beta$ , which corresponds to the poles of the Hamiltonian (3.6). Note that it is no longer the case that every crossing curve contains a pole. This means that crossing anywhere on the curve yields the same generator of the braid word, i.e. the entire curve is a single generator arc.

**§4.5 An array example.** We now perform the calculations described in §4.4 on the array case shown in Figure 3.2. See [SA] for a details on this and other array examples. The crossing curves corresponding to  $s_1$  and  $s_3$  are defined by  $\text{Re}(\psi_1(Z)) = \text{Re}(\psi_3(Z))$ , which, writing  $Z = x + iy$ , is

$$\exp(-2\pi y) \cos(2\pi x) = \exp(-2\pi(\frac{2}{3}y - \frac{1}{4})) \cos(2\pi(\frac{2}{3}x - \frac{1}{12})).$$

Both cosine terms can vanish yielding the two vertical lines  $x = 5/4$  and  $x = 11/4$ . Otherwise we may solve for

$$y = \frac{3}{2\pi} (\log(\frac{\cos(2\pi x)}{\cos(2\pi(\frac{2}{3}x - \frac{1}{12}))}) - \pi/2)$$

which is defined only on the (mod 3) intervals  $(-3/4, 1/4)$ ,  $(1/2, 3/4)$ , and  $(7/4, 2)$ . Thus there are five distinct  $(1, 3)$ -crossing curves. The computations for other pairs is similar and the various crossing curves are shown in Figure 4.3a. The numbers separated by a hyphen indicate which pair of  $s_\alpha$ 's are crossing. Note that since the vertical lines  $x = 5/4$  and  $x = 11/4$  correspond to  $0 = \text{Re}(s_1) = \text{Re}(s_3)$ , and we are considering 0 as the position of  $s_4$ , these vertical lines correspond to a triple crossing.

The poles are the points 0, 1 and 2 corresponding to  $s_1 = s_2$ , the points  $\frac{1}{8} + \frac{3}{8}i$  and  $\frac{13}{8} + \frac{3}{8}i$  corresponding to  $s_2 = s_3$ , and the point  $-\frac{1}{4} - \frac{3}{4}i$  corresponding to  $s_1 = s_3$ . Note that many crossing curves do not contain a pole. Figure 4.3b shows the results of computing the generator arcs, with labels using the same conventions as in Figure 4.1.

It is important to note that the details of Figure 4.3 are not intrinsic to the vortex motions. Changing the projection plane used to compute the braids would change all the crossing curves. However, the braid which is computed for a loop is intrinsic up to conjugacy. In algebraic language, after fixing a basepoint, the equations (4.4) (using  $Z(t)$  to represent a general loop) may be used to define a homomorphism of  $\pi_1(R - \{\text{poles}\}) \rightarrow B_4$ . This homomorphism is not intrinsic, but it is intrinsic up to conjugacy in  $B_4$ .

Now define a regime as in the planar case, i.e. as a connected component of  $R - \{\text{poles and separatrices}\}$ . Each periodic orbit in a regime gives rise to the same mathematical braid; these are listed in the second column of Table 4.1. Note that the relations in the braid group have been used to simplify many of the braid words. The braids for regimes I and IX through XIII were computed using closed trajectories with initial position near the point labelled  $r$  in Figure 4.3b. The initial position used for regime II was near the point labelled  $q$ .

As a sample we compute the mathematical braids corresponding to regimes I and XIII. The closed orbits in regime I travel across the top of the reduced plane from left to right. To

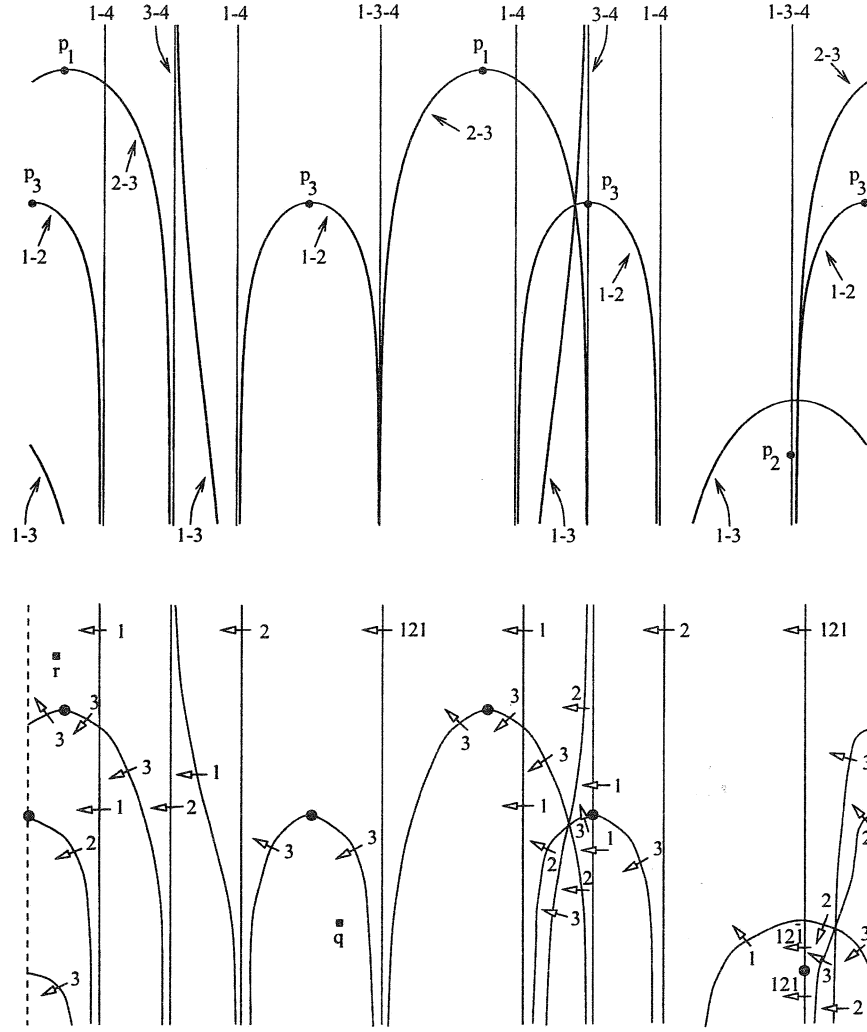


**Figure 4.3:** (a) Crossing curves and (b) generator arcs for the system in Figure 3.2 (the picture in (b) has been distorted for increased clarity). The points labelled  $q$  and  $r$  correspond to initial points of trajectories as explained in the text.

compute the braid we chose the point labeled  $r$  in Figure 4.3b as the initial point. Moving to the right from this point we first traverse a vertical line on which there is an arrow labeled 1. This indicates that the motion of the trajectory has resulted in a crossing of the two left most strands in the physical braid representing the vortices. Further, since the trajectory's motion is opposite to that of the arrow, the strands are crossing with the left one in front of the right one. Thus the traversing of the first crossing curve contributes the letter  $\bar{\sigma}_1$  to the braid word of the trajectory. Continuing to the right the trajectory traverses a crossing curve on which there is an arrow labeled 2 and the arrow points in the direction opposite to the traverse. Thus this motion contributes a  $\bar{\sigma}_2$  to the braid word of the trajectory. Continuing across the top of Figure 4.3b, we add braid letters  $\bar{\sigma}_1$ , then  $\bar{\sigma}_2$ , etc. After encountering the right edge of the phase plane the identification with the left edge allows a return to the initial point. The entire braid word for this regime is thus

| Regime | Braid   | TN type             | Expansion Constant |
|--------|---|---------------------|--------------------|
| I      | $(\bar{\sigma}_1 \bar{\sigma}_2)^3 \bar{\sigma}_1^2 (\bar{\sigma}_2 \bar{\sigma}_1)^3$  | reducible, all f.o. |                    |
| II     | $\sigma_3 \sigma_2 (\sigma_1 \sigma_2 \sigma_3)^2 \sigma_2 \sigma_3 \sigma_1 \sigma_2 \sigma_1 (\sigma_1 \sigma_2 \sigma_3)^2 \sigma_2 \sigma_1 \sigma_3 \sigma_1 \sigma_2 \sigma_1 \sigma_3$ | reducible, all f.o. |                    |
| III    | $\sigma_3^2$  | reducible, all f.o. |                    |
| IV     | $\sigma_3^2$  | reducible, all f.o. |                    |
| V      | $\sigma_1^2$  | reducible, all f.o. |                    |
| VI     | $\bar{\sigma}_2^2$  | reducible, all f.o. |                    |
| VII    | $\sigma_3^2$  | reducible, all f.o. |                    |
| VIII   | $\bar{\sigma}_3^2$  | reducible, all f.o. |                    |
| IX     | $\sigma_3^2 \sigma_2^2$   | reducible, all f.o. |                    |
| X      | $(\sigma_3 \sigma_2)^3$   | reducible, all f.o. |                    |
| XI     | $(\sigma_3 \sigma_2)^2 \sigma_3 \sigma_1 \sigma_2 \sigma_1^2 \sigma_2 \sigma_1 \sigma_2 \sigma_3 \sigma_1 \sigma_3 (\bar{\sigma}_1 \bar{\sigma}_2)^3 \bar{\sigma}_1$                          | pA                  | 13.93              |
| XII    | $(\sigma_3 \sigma_2)^2 \sigma_3 \sigma_1 \sigma_2 \sigma_1^2 (\sigma_2 \sigma_3 \sigma_1 \sigma_3)^2 (\bar{\sigma}_1 \bar{\sigma}_2)^3 \bar{\sigma}_1$  | reducible, one pA   | 13.93              |
| XIII   | $(\bar{\sigma}_1 \bar{\sigma}_2)^2 \bar{\sigma}_3^2 (\bar{\sigma}_2 \bar{\sigma}_1)^5$  | pA                  | 9.90               |

**Table 4.1:** The mathematical braids and Thurston-Nielsen type of the regimes for the system shown in Figure 3.2. The expansion constants for pseudoAnosov (pA) components are given. In the finite order (f.o.) case these constants are 1. This means that there is no intrinsic topological expansion in that case.

$$\bar{\sigma}_1 \bar{\sigma}_2 \bar{\sigma}_1 \bar{\sigma}_2 \bar{\sigma}_1 \bar{\sigma}_2 \bar{\sigma}_1 \bar{\sigma}_1 \bar{\sigma}_2 \bar{\sigma}_1 \bar{\sigma}_2 \bar{\sigma}_1 \bar{\sigma}_2 \bar{\sigma}_1 = (\bar{\sigma}_1 \bar{\sigma}_2)^3 \bar{\sigma}_1^2 (\bar{\sigma}_2 \bar{\sigma}_1)^3.$$

The closed trajectories for regime XIII have a motion similar to those of regime I with the crucial topological difference that they pass below the pole  $p_3$  which is located at  $1 + 0i$ . This implies that in the complement of the poles, the closed loops corresponding to regimes I and XIII are *not* homotopic. Beginning a closed trajectory representing regime XIII near the point  $r$ , the braid word starts with  $\bar{\sigma}_1 \bar{\sigma}_2 \bar{\sigma}_1 \bar{\sigma}_2$  like that of regime I, but since the loops for regime XIII pass below the point  $p_3$ , their braid words have a  $\bar{\sigma}_3 \bar{\sigma}_3$  next, and then continue with the same letters as regime I. The entire braid word for regime XII is thus  $\bar{\sigma}_1 \bar{\sigma}_2 \bar{\sigma}_1 \bar{\sigma}_2 \bar{\sigma}_3 \bar{\sigma}_3 \bar{\sigma}_1 \bar{\sigma}_2 \bar{\sigma}_1 \bar{\sigma}_1 \bar{\sigma}_2 \bar{\sigma}_1 \bar{\sigma}_2 \bar{\sigma}_1 \bar{\sigma}_2 \bar{\sigma}_1$ . Note that the braid relation  $\bar{\sigma}_1 \bar{\sigma}_2 \bar{\sigma}_1 = \bar{\sigma}_2 \bar{\sigma}_1 \bar{\sigma}_2$  used on the triple of letters right after the  $\bar{\sigma}_3 \bar{\sigma}_3$  allows us to reduce the word to  $(\bar{\sigma}_1 \bar{\sigma}_2)^2 \bar{\sigma}_3^2 (\bar{\sigma}_2 \bar{\sigma}_1)^5$  as given in Table 4.1.

We now briefly describe some of the motions. In these descriptions we will use the word “vortex” to refer to the trajectories of the planar motions,  $s_1, s_2, s_3$ , and  $s_4$ . Properly speaking  $s_1, s_2$ , and  $s_3$  are the transformed positions of the vortices, and  $s_4$  is not a vortex at all, but rather it keeps track of the position of the origin.

Before interpreting the braid, it is useful to recall the various transformations that have been used. The motion in the singly periodic plane is really of infinite families of vortices. These families are treated as three individual vortices on a cylinder and then this motion is transformed to the punctured plane. Thus a strand in the braid rotating about the strand representing vortex 4 (= the origin) describes motion around the cylinder, which in turn, is a horizontal translation by one period of the corresponding family of vortices in the singly-periodic plane. In addition, the braid is obtained using the frame of the second vortex, so in particular vortex 2 will never rotate around the origin, and thus the strands corresponding to vortex 2 and 4 will always be parallel.

The regimes with the simplest braids are those that contain a pole, III through VIII. The vortex motions are topologically the same as regions A, B, and C in the plane case: a pair of vortices are circling each other and the other vortex is uninvolved. There is no rotation around the origin, thus there is no net rotation around the cylinder.

The vortex motions corresponding to regime X also have no net motion around the cylinder (see figure 6.1a). This is indicated by the fact that none of the other strands link with the far left one which represents the origin of  $\mathbb{C}$ . Examining the right hand sub-braid on 3 strands, one sees that every vortex rotates about every other one once in the clockwise direction. The net motion is the same as that in the planar region D and it amounts to one full rotation of the vortices as a group. The motions in regime IX are similar, but the sub-braid is slightly different; vortices 2 and 3 rotate about each other clockwise, and then vortices 1 and 3 do likewise, but vortices 1 and 2 do not link.

The regimes with the next simplest braids are I and II. The mathematical braid for I is shown in Figure 4.4d. Vortex 1 rotates three times around the origin counter clockwise and vortex 3 rotates twice, also counter clockwise. This rotation takes place “inside” the fixed vortex 2. In the singly periodic plane, this corresponds to the vortex 1 family translating three strips to the right and the vortex 3 family two strips; this translation takes place below the position of vortex 2. This motion is shown in Figure 4.4a with one vortex from each singly periodic family pictured. Figure 4.4b shows the motion in the frame of the second vortex after it has been transformed to the plane. The physical braid of this motion constructed using (4.4) and (4.2) is shown in Figure 4.4c. The motion in regime II is similar, but now the rotation is clockwise, and goes around vortex 2, which simply means that in the singly-periodic plane the translations of vortex 1 and 3 are above the position of vortex 2.

The motion in regimes XI, XII, and XIII is sufficiently complicated that the braid itself is the best description of the motion. One feature of interest in regime XII (see Figure 6.1b) is that the vortex pair 1 and 3 have the same motion with respect to the other two strands while they rotate about each other three times. This kind of hierarchy of motion is described precisely by the notion of reducibility introduced in §5.

**§4.6 Three-vortex lattices.** The method of analysis of this section can also be applied to vortex lattices. When  $\Gamma_3 = p/q$  is rational, the reduced Hamiltonian system (3.6) can be viewed as taking place on a torus with width  $p$  in both directions. The generic orbit of this system will be a periodic orbit  $Z(t)$ . This periodic orbit can be used to generate a motion of the three vortices on the torus which will be periodic in the frame of one of the vortices. However, in contrast to the array case, this cannot be transformed into a motion on the plane, and so one must record the motion using the braid group of the torus. This group not only has generators corresponding to the switching of two points as in the usual braid group, but it also has generators describing motions that circulate around the meridian and longitude of the torus (see [Bm2]). Thus the braids are more difficult to visualise. However the basic features of the analysis in the array and plane case go through with no difficulty. In particular, each regime is assigned just one braid, and so the braid captures the sense in which all the vortex motions in one regime are topologically the same and distinct from those of other regimes.

## §5 Isotopy classes and the Thurston-Nielsen theory.

This section provides an introduction to isotopies and the Thurston-Nielsen theory in preparation for the study of the advection homeomorphisms generated by vortex motions.

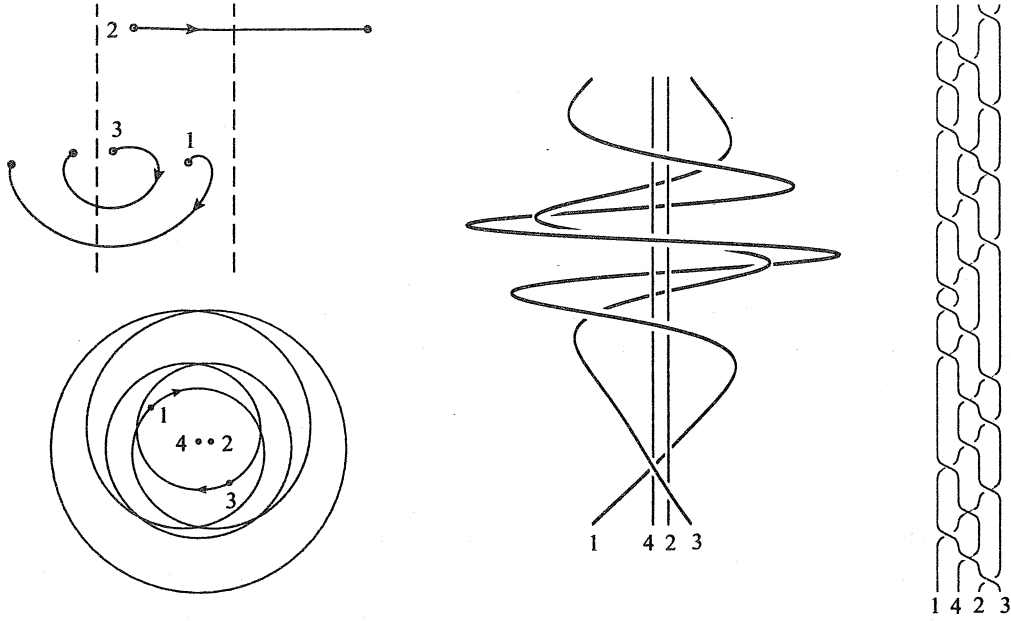


**Figure 4.4:** Vortex motion from regime II of Figure 3.2. (a) Trajectories of the three vortices in the singly-periodic plane (only one representative of each family is shown). (b) The motion in the frame of the second vortex transformed into the plane. (c) Physical braid of the transformed motion. (d) Mathematical braid of the transformed motion.

Roughly speaking, two homeomorphisms are isotopic if one is a continuous deformation of the other. The braid of a vortex motion will be seen to determine the isotopy class of the corresponding advection homeomorphism. The braid is then used as input into the Thurston-Nielsen theory which describes dynamical data that is shared by isotopic homeomorphisms, and is thus present in the advection homeomorphism.

**§5.1 Homeomorphisms, isotopy, and braids.** A one-to-one and onto map  $f : X \rightarrow X$  is called a *homeomorphism* if  $f$  and its inverse,  $f^{-1}$ , are both continuous. If in addition,  $f$  and  $f^{-1}$  are both differentiable, then  $f$  is called a *diffeomorphism*. Two homeomorphisms  $f$  and  $g$  are *conjugate* if there is a third homeomorphism  $h$  with  $f = hgh^{-1}$ . The homeomorphism  $h$  represents the change of coordinates from  $f$  to  $g$ . If  $E$  is a finite set and  $f(E) = E$ , then  $f$  is called a *rel  $E$  diffeomorphism* or *homeomorphism*.

Most of the homeomorphisms occurring in this paper are defined using the advection of a passive particle in a time varying velocity field. Given a vector field on the plane  $(u, v)$ , the advection equations are

$$\frac{dx}{dt} = u(x, y, t) \quad \frac{dy}{dt} = v(x, y, t). \quad (5.1)$$

Letting  $z = (x, y)$ , the solution with position  $z_0$  at time  $t_0$  is denoted  $z(t; z_0, t_0)$ . By convention the running time  $t$  satisfies  $z(t_0; z_0, t_0) = z_0$ , *not*  $z(0; z_0, t_0) = z_0$  (unless, of course,  $t_0 = 0$ ). Fixing a time  $t$ , the *time  $t$ -flow map* or the *time  $t$ -advection homeomorphism* is defined as  $h_t(z_0) := z(t; z_0, 0)$ , i.e. we advect each particle for time  $t$ , and  $h_t$  maps each initial position to its final position. The collection of  $h_t$  for all  $t$  describes all the solutions

and is called a *fluid motion* (cf. §3.1 on the use of “flow”). Note that given a fluid motion the underlying velocity field is obtained by differentiation.

The usual definition of isotopy rel a finite set  $E$  is the following. Given two rel  $E$  homeomorphisms  $f_i : \mathbb{R}^2 \rightarrow \mathbb{R}^2$ , say that  $f_0$  is *isotopic to  $f_1$  rel  $E$*  if they can be connected by a continuous family of rel  $E$  homeomorphisms  $f_t$ ,  $t \in [0, 1]$ . Since  $E$  is a finite set this implies that  $f_t(k) = f_0(k)$  for all  $t$  and  $k \in E$ . The collection of *homeomorphisms* isotopic to  $f$  rel  $E$  is called its *rel  $E$  isotopy class*. The finite set  $E$  in the sequel will be the initial positions of the collection of point vortices. These points will be fixed under the advection homeomorphism considered, but in general, the points of  $E$  could be permuted by a rel  $E$  homeomorphism. It is sometimes convenient to remove the set  $E$  from the plane and consider a rel  $E$  homeomorphism as a homeomorphism of the punctured plane  $\mathbb{R}^2 - E$ . Note that two rel  $E$  homeomorphisms are isotopic rel  $E$  exactly when they are isotopic as homeomorphisms of  $\mathbb{R}^2 - E$ .

The exposition of isotopy in fluid mechanical terms is most clear in the special case of isotopy to the identity rel  $E$ . For simplicity we restrict to the case of diffeomorphisms as is natural for fluid mechanical applications. A rel  $E$  diffeomorphism  $f : \mathbb{R}^2 \rightarrow \mathbb{R}^2$  will be isotopic to the identity rel  $E$  exactly when  $f$  is the time 1 advection homeomorphism of a velocity field which satisfies  $u(k, t) = v(k, t) = 0$  for all  $k \in E$  and  $t \in [0, 1]$ . This means that all the points of  $E$  are fixed throughout the advection. Thus we may think of  $f$  as arising from advection due to body forces on the fluid and the points in  $E$  as fixed point-like regions that are not permeable by the fluid. If the points of  $E$  move under a given fluid motion, the time-one flow map can still be isotopic to the identity if there is *another* fluid motion that also gives rise to  $f$ , but in this new motion the points of  $E$  are fixed for the entire motion.

The braid associated with the motion of points in  $E$  can be used to determine whether a given advection diffeomorphism is isotopic to the identity. Given a fluid motion  $h_t$ , the motion of the points in  $E$  is given by  $a_i(t) := h_t(k_i)$  for each  $k_i \in E$ . Now a family of diffeomorphisms  $\psi_t : \mathbb{R}^2 \rightarrow \mathbb{R}^2$  for  $t \in [0, 1]$  with  $\psi_t(a_i(t)) = k_i$  for all  $k_i \in E$  and  $\psi_0 = \psi_1 = id$  induces a level preserving diffeomorphism  $\Psi : \mathbb{R}^2 \times [0, 1] \rightarrow \mathbb{R}^2 \times [0, 1]$  defined by  $\Psi(z, t) = (\psi_t(z), t)$ . The diffeomorphism  $\Psi$  will take  $\mathbf{b}$  to the trivial physical braid which consists of just vertical strands at the points of  $E$ . If this is the case say that  $\mathbf{b}$  is weakly equivalent to the trivial braid  $\mathbf{b}_{triv}$ .

The relationship of braids to isotopy classes is this: given a fluid motion  $h_t$  with advection homeomorphism  $f = h_1$  and a finite set  $E$  with  $f(E) = E$ , then  $f$  is isotopic to the identity rel  $E$  if and only if the physical braid  $\mathbf{b}$  describing the motion of  $E$  is weakly equivalent to  $\mathbf{b}_{triv}$ . Here is the proof. If  $\mathbf{b}$  is weakly equivalent to  $\mathbf{b}_{triv}$  by the family  $\psi_t$ , then  $h'_t = \psi_t \circ h_t$  is a fluid motion that fixes  $E$  for all  $t \in [0, 1]$  and  $h'_1 = h_1 = f$ , and so  $f$  is isotopic to the identity. Conversely, if  $h'_t$  is a fluid motion that fixes  $E$  for all  $t \in [0, 1]$  and  $h'_1 = h_1 = f$ , then  $\psi_t = h'_t \circ h_t^{-1}$  is a family that will make  $\mathbf{b}$  weakly equivalent to  $\mathbf{b}_{triv}$ .

The next step is to see how the braid word describing the motion of  $E$  indicates when the advection diffeomorphism is isotopic to the identity rel  $E$ . This is certainly the case when the mathematical braid is the identity element in the braid group, but this is not the only case. Consider the plane motion given in complex coordinates by  $h_t(z) = |z| \exp(2\pi it)$ . For a given  $n$ , let  $E$  be the set of  $n^{th}$  roots of unity,  $\{\exp 2\pi i j/n : j = 1, \dots, n\}$ . Then it is easy to check that the physical braid  $\mathbf{b}$  of the motion of  $E$  has a mathematical braid  $(\bar{\sigma}_1 \bar{\sigma}_2 \dots \bar{\sigma}_{n-1})^n$  and further that the diffeomorphism  $\Psi(z, t) = (|z| \exp(-2\pi it), t)$  makes  $\mathbf{b}$  weakly equivalent to  $\mathbf{b}_{triv}$ . It is known that this mathematical braid and its powers are the



only cases where this happens ([Bm1]). More precisely, if we let  $\hat{B}_n$  be  $B_n$  with the added relation that  $(\sigma_1\sigma_2 \dots \sigma_{n-1})^n$  is the identity element, then the braid word of  $\mathbf{b}$  is equivalent to the identity element of  $\hat{B}_n$  exactly when  $\mathbf{b}$  is weakly equivalent to  $\mathbf{b}_{triv}$ . Note that the center of  $B_n$  (i.e. all the elements which commute with every other element) is exactly all the powers of  $(\sigma_1\sigma_2 \dots \sigma_{n-1})^n$ , so one could more succinctly define  $\hat{B}_n$  as  $B_n$  mod its center.

For  $n > 2$ ,  $\hat{B}_n$  has infinitely many elements, and so there are many diffeomorphisms that are not isotopic to the identity; the simplest example is when  $E$  is three points and  $F$  is a rel  $E$  diffeomorphism with mathematical braid  $\sigma_1^2$ . When diffeomorphisms are not isotopic to the identity, isotopy can be described using the identity case as follows. Two rel  $E$  diffeomorphisms  $f$  and  $g$  are isotopic if there is third diffeomorphism  $h$ , with  $h$  isotopic to the identity, and  $g = h \circ f$ . If  $f$  and  $g$  are time one maps of fluid motions, this says that they are isotopic if we can accomplish the same advection as  $g$  by first allowing the advection for  $f$  and then following it by a fluid motion that keeps the points of  $E$  fixed.

The connection of braids to this more general notion of isotopy requires the general definition of weakly equivalent physical braids. Two physical braids  $\mathbf{b}^0$  and  $\mathbf{b}^1$ , both with endpoints  $E$  are weakly equivalent if there is a level preserving diffeomorphism  $\Psi : \mathbb{R}^2 \times [0, 1] \rightarrow \mathbb{R}^2 \times [0, 1]$  that takes  $\mathbf{b}^0$  to  $\mathbf{b}^1$  where  $\Psi(z, t) = (\psi_t(z), t)$  for some family of diffeomorphisms  $\psi_t$  with  $\psi_0 = \psi_1 = id$ . Using the result in the identity case, we have that two rel  $E$  advection diffeomorphisms are isotopic if and only if their physical braids with endpoints  $E$  are weakly equivalent which happens if and only if the corresponding braid words are equivalent in  $\hat{B}_n$ . In different language, the collection of rel  $E$  isotopy classes forms a group under composition; this group is isomorphic to  $\hat{B}_n$ , where  $n$  is the number of elements in  $E$ .

It is worth noting that when two physical braids with endpoints  $E$  are equivalent in the sense defined in §4.1, they are weakly equivalent (hence the use of the modifier “weakly”). This is easily seen using the corresponding mathematical braids. The equivalent physical braids have the same braid word in  $B_n$ , and hence in  $\hat{B}_n$ , and thus they are weakly equivalent. The converse need not be true, the simplest example being the trivial braid and a physical braid having braid word  $(\sigma_1\sigma_2 \dots \sigma_{n-1})^n$ . These represent the same word in  $\hat{B}_n$ , but not in  $B_n$ , and hence the physical braids are weakly equivalent but not equivalent.

The last step is to extend these ideas to allow different distinguished sets  $E$  so that vortex motions with different initial configurations can be compared. A rel  $E$  diffeomorphism  $f$  and a rel  $E'$  diffeomorphism  $f'$  are *isotopic up to conjugacy* if there is a homeomorphism  $h$  with  $h(E') = E$  and  $hf'h^{-1}$  is isotopic to  $f$  rel  $E$ . Thus  $f$  and  $g$  are isotopic after a change of coordinates. Two physical braids  $\mathbf{b}$  and  $\mathbf{b}'$  with endpoints  $E$  and  $E'$  are weakly equivalent if there exists a diffeomorphism  $h : \mathbb{R}^2 \rightarrow \mathbb{R}^2$  with  $h(a_i(0)) = a'_i(0)$  for all  $i$  (and so  $h(E) = E'$ ) and the physical braid  $\{(h(a_i(t)), t)\}$  is weakly equivalent to  $\mathbf{b}'$ . We then have that two advection diffeomorphisms are isotopic up to conjugacy if and only if their physical braids are weakly equivalent, which happens if and only if their mathematical braid words are conjugate in  $\hat{B}_n$ .

**§5.2 The Thurston-Nielsen representative.** The Thurston-Nielsen theory provides tools to analyse homeomorphisms using their isotopy classes. The theory constructs in each isotopy class a special homeomorphism which is now called the Thurston-Nielsen (TN) representative. This TN-homeomorphism is in a precise sense the simplest map in the isotopy class. Simplest here means in both the topological and dynamical sense. Thus once we understand the topology and dynamics of the TN-homeomorphism in an isotopy class, we know

dynamical and topological complexity that must be present in *every* homeomorphism in the class. This subsection and the next contain an introduction to the Thurston-Nielsen theory that is targeted for our applications. In particular, only homeomorphisms of the punctured plane are considered here, or equivalently, homeomorphisms of the plane rel a finite set  $E$ . The Thurston-Nielsen theory holds for the much wider class of surfaces of negative Euler characteristic. The reader is urged to consult [T], [FLP] or [CB] for a more balanced and complete treatment. For a survey of the dynamical applications of the Thurston-Nielsen theory, see [Bd].

The TN-homeomorphisms are of three basic types. The first type consists of dynamically very simple maps called *finite order (fo)*. These are defined by the property that for some  $m > 0$  the map composed with itself  $m$  times equals the identity map. The second type of TN-homeomorphisms are dynamically very complicated and are called *pseudoAnosov (pA)* homeomorphisms. These will be discussed in greater detail in the next subsection because the presence of a pA homeomorphism in an isotopy class has strong implications for the dynamics of an advection homeomorphism. The final type of TN-homeomorphisms are *reducible*, which means that there is a collection of simple disjoint loops with the property that the loops are permuted by the reducible homeomorphism. Cutting along the loops yields a collection of smaller surfaces and on each of these surfaces the reducible homeomorphism is either finite order or pseudoAnosov.

A given isotopy class can only contain a TN-map of one type, and thus an isotopy class is called pseudoAnosov, finite order or reducible depending on what kind of TN-map it contains. Note that the conjugate of a TN-map is also a TN-map of the same type. Thus, using the results of the previous subsection, one may also speak of the TN-type of a braid or a braid type. There are many theorems which help decide the TN-type of a braid or isotopy class. Rather than catalog these results here it will suffice to note that there is a computer implementation of an algorithm due to Bestvina and Handel ([BH]) (cf. [FM] and [Ls]) which, given the braid word, decides the TN-type. In the pA case the algorithm outputs the isotopy invariant dynamical data described in the next subsection.<sup>1</sup>

For planar regions the finite order braids and rel  $E$  isotopy classes are well known. If we let  $R_n$  denote rigid rotation of the plane by  $-2\pi/n$ , then certainly  $R_n^n = id$ , and so  $R_n$  is finite order. We may consider  $R_n$  as the time one flow map of the motion given in complex coordinates by  $h_t(z) = -|z|\exp(2\pi it/n)$ . If  $E$  is the set of  $n^{th}$  roots of unity, its physical braid under this motion is  $\beta_n := \sigma_1 \sigma_2 \dots \sigma_{n-1}$ . Note that  $\beta_n^n$  is the identity element of  $\hat{B}_n$ , and making this property hold is, in fact, the defining feature of  $\hat{B}_n$ . Thus  $\beta_n$  is a finite order braid and so is  $\beta_n^m$  for any  $0 \leq m \leq n-1$ . A classic result of Brouwer (see section 8.2 in [Bd]) says that all finite order homeomorphisms of the plane are conjugate to rigid rotations. This implies that the  $\beta_n^m$  are the only finite order braids on  $n$  strands. Examples of other braids with various TN-types are given with vortex examples in §6.2.

For planar regions the Thurston-Nielsen theory only has content for regions having three or more punctures or holes, or equivalently, for isotopy classes rel three or more points. When  $E$  contains just two points, all TN-homeomorphisms are finite order since  $\hat{B}_2$  only contains the identity element  $e$  and the braid  $\sigma_1$  with  $\sigma_1^2 = e$ . Classic results of Alexander (see Cahpetr XV in [D]) say that when  $E$  has one or zero elements, there is only one isotopy

---

<sup>1</sup> There is a C++ implementation of this algorithm by Toby Hall (with a Win95 interface) available for download. Contact the first author for site locations.

class; all orientation preserving homeomorphisms of the plane are isotopic, as are those of the once punctured plane.

**§5.3 PseudoAnosov maps and isotopy classes.** Linear Anosov maps on tori provide one of the best known and understood examples of chaotic dynamics. The homeomorphism  $\phi$  of the two torus induced by the matrix

$$M = \begin{pmatrix} 2 & 1 \\ 1 & 1 \end{pmatrix}$$

acting on the plane is called Thom's toral automorphism or Arnolds' cat map, the latter nomenclature derived from an illustration in [AA]. The homeomorphism  $\phi$  has a Markov partition with transition matrix  $M$  that gives a symbolic description of the dynamics. The largest eigenvalue  $\lambda > 1$  of  $M$  controls much of the dynamical asymptotics. The number of fixed points of  $\phi^n$  grows like  $\lambda^n$  as does the length of topologically nontrivial loops under iteration. In addition, these properties are shared in the appropriate sense by any homeomorphism on the torus that is isotopic to  $\phi$  ([Fk]).

For the map  $\phi$  there is uniform stretching and contraction by  $\lambda$  at every point, and the corresponding eigendirections fit together to yield a pair of foliations of the torus by unstable and stable manifolds. Such nonsingular foliations cannot live on surfaces of negative Euler characteristic like the multi-punctured plane, and thus these surfaces cannot support Anosov maps. However, pseudoAnosov maps do exist on these surfaces and share many of the properties of Anosov maps.

In pseudoAnosov maps there is still uniform stretching and contracting at each point by a factor  $\lambda$ . The unstable and stable directions still fit together into invariant unstable and stable foliations but these foliations must have a finite number of points (called singularities or prongs) where there is either one or three or more stable directions and the same number of unstable directions. Despite the presence of these singularities, pseudoAnosov maps share most of the basic properties of Anosov maps. There is a Markov partition with transition matrix  $M$  that allows one to code the dynamics of the pA map  $\phi$ . The largest eigenvalue of  $M$  is the stretching factor  $\lambda > 1$ . The number of fixed points of  $\phi^n$  grows like  $\lambda^n$  as does the length of topologically nontrivial loops under iteration. The precise way in which these properties are shared by any isotopic map is described by the following theorem due to Handel ([H]). The notation  $g|_Y$  means the map  $g$  restricted to the set  $Y$ .

**Theorem:** *If  $\phi : M^2 \rightarrow M^2$  is a pseudoAnosov homeomorphism and  $g$  is isotopic to  $\phi$ , then there exists a closed,  $g$  invariant set  $Y$ , and a continuous, onto map  $\alpha : Y \rightarrow M^2$ , so that  $\alpha \circ g|_Y = \phi \circ \alpha$ . Further, for any periodic point  $x$  of  $\phi$ , there is a periodic point of the same period  $y$  of  $g$  with  $\alpha(y) = x$ .*

Thus any map  $g$  isotopic to a pA map has a compact invariant set that is semiconjugate to the pA map. Since the map  $\alpha$  is onto, the dynamics of  $g$  are at least as complicated as those of the pA map  $\phi$ . Thus, for example, the exponential growth rate of the number of fixed points of  $g^n$  is at least  $\lambda$  and the topological entropy of  $g$  is greater than or equal to  $\log(\lambda)$ . Note that nothing prevents the dynamics of  $g$  from being more complicated than that of  $\phi$ , the theory provides just a lower bound.

A loop in a surface is called topologically nontrivial if it cannot be deformed into a point, a puncture, or a boundary component. Another basic result about pA maps is that the length

of topologically nontrivial loops grows like  $\lambda^n$  under iteration. Via the semiconjugacy, this implies a similar growth under  $g$ . It is important to note that this does not imply that the map  $g$  has Lyapunov exponents equal to  $\log(\lambda)$  everywhere. One does obtain from smooth ergodic theory that  $g$  has an ergodic invariant measure with an exponent at least  $\log(\lambda)$  (cf. [KH]), but this measure will be supported on the set  $Y$ , which could be small with respect to the usual measure on  $M$ .

Since the number  $\lambda$  can be computed by the Bestvina-Handel algorithm, the braid describing an isotopy class yields quantitative information about any homeomorphism in the isotopy class. An example of an isotopy class containing an advection homeomorphism induced by vortex motion is given §6.3. The Bestvina-Handel algorithm also returns a one dimensional graph called a *train track* in addition to a self-transformation of the graph. The edges of the graph form the Markov partition for the pA map, and the self-transformation of the graph provides the transition matrix as well as the structure of the invariant foliations. These foliations are sometimes called the “invariant manifold template” of the pA map. The semiconjugacy then gives a lower bound or skeleton for the invariant manifold templates of  $g$ .

## §6 Advection and isotopy classes.

In this section we use the Thurston-Nielsen theory to study the of advection of a passive particle in the velocity field produced by three point vortices. In §6.1 a Poincaré map (or advection homeomorphism) is defined whose iterates describes the dynamics of passive scalars. This is a standard construction, but an adjustment is required because of the dynamic phase in the periodic motion of the vortices. In §6.2 we study isotopy classes of the advection homeomorphisms in the plane and array case using the braids computed in §4. Since all the motions in a single regime have the same braid, all the corresponding advection homeomorphisms have the same TN type. For the planar case, these are all reducible or finite order, but the array case has regimes of pA type. In §6.3 we study one such pA regime in detail.

**§6.1 The Poincaré map.** As we have seen, a vortex motion  $z_\alpha(t)$  can be obtained by solving (2.1) directly, or as in §3, by using (3.4) and a period  $P$  solution  $Z(t)$  of the reduced equations (3.5). The vortex motion, in turn, generates a velocity field given by the right hand side of (2.3). The goal of this subsection is to define a Poincaré map. The iterates of this map will describe the time evolution of passive particles advected in this velocity field. There is a standard construction of such a map for an equation of the form  $\dot{z} = F(z, t)$  with  $F$  a velocity field  $P$ -periodic in  $t$ . The time- $P$  flow map  $f$  as defined in §5.1 by  $f(z_0) = z(P; z_0, 0)$  will satisfy  $f^n(z_0) = z(nP; z_0, 0)$ , and so the iterates of  $f$  describe the time evolution of points in discrete steps of size  $P$ .

For the advection caused by the point vortices this construction needs to be altered slightly because the vortex trajectories satisfy  $z_\alpha(t + P) = z_\alpha(t) + b$ , with  $b$  the dynamic phase associated with  $Z(t)$ . The easiest alteration is to pass to a uniformly translating frame with velocity  $b/P$ . If  $F(z, t)$  denotes the right hand side of (2.3) corresponding to the given vortex motion, define the *advection homeomorphism*  $f$  as the time  $P$ -flow map of the equation

$$\dot{\zeta} = F\left(\zeta + \frac{b}{P}t, t\right) - \frac{b}{P}.$$

This advection homeomorphism satisfies  $f^n(z_0) = z(nP; z_0, 0) - nb$ , and so  $f$  describes the position of a particle after advecting for one period  $P$  and then translating by  $-b$ .

Alternatively, this could have been taken as the definition of  $f$ , i.e.  $f(z_0) = z(P; z_0, 0) - b$  with  $z$  the solution of (2.3). Points that are periodic under  $f$  correspond to advected particles that are translating along with the vortices, but after some integer multiple of  $P$  they have returned to their initial positions relative to the vortices. Although the velocity field is not defined at the positions of the vortices, the homeomorphism  $f$  can be extended (continuously, not differentially) to make the three initial positions of the vortices,  $z_\alpha(0)$ , fixed points.

In §4.3 the motion of a vortex array in the cylinder was transformed to the plane minus the origin by the conformal map  $T$ . The advection homeomorphism in this case is transformed to  $\hat{f} = T f T^{-1}$ . Note that  $\hat{f}$  may be extended to make 0 a fixed point. Thus all the  $s_\alpha(0)$  from (4.4) can be considered as fixed points of  $\hat{f}$ .

**§6.2 The TN type of regimes.** As seen in §4.2 and §4.4, all the periodic orbits in the same regime in the reduced plane give rise to the same braid. By results in §4.1 this implies that all the corresponding advection homeomorphisms have the same braid type, which allows us to speak of the TN type of a regime. If this type is pA, then as in §5.3 all the advection homeomorphisms will share a certain set of dynamics.

In the case of three vortices in the plane, only two braid types arose as descriptions of regimes. In one of them, a pair of vortices rotate around one other while the other vortex is uninvolved. This is a reducible class, with a finite order component containing the pair of interacting vortices. The other regime, D, had braid  $(\sigma_1 \sigma_2)^3$ , which is the identity element in  $\hat{B}_3$ , and the advection homeomorphism in this case is isotopic to the identity, with the isotopy consisting of unwrapping the plane via single rotation; this topologically undoes whatever advection was caused by the vortices. Since only pA classes or components yield dynamical information from the Thurston-Nielsen theory, the theory gives no information about advection dynamics in the planar case.

The Thurston-Nielsen theory does provide dynamical information about advection induced by vortex arrays. The Bestvina-Handel algorithm was used to compute the TN type of the various regimes from Figure 3.2. Using the braids given in the second column as input, the computed TN type is shown in the third column of Table 4.1. When a regime is pA (or has a pA component), the expansion constant is given in the right column.

As we comment on the various regimes the reader is urged to draw a picture of the appropriate braids. The regimes which contain poles, III through VIII, correspond to a pair of vortices which rotate around one other while the other is uninvolved. As in the planar case, the isotopy classes of the advection homeomorphisms are reducible with a finite order component containing the pair of interacting vortices.

In the braid for regime X shown in Figure 6.1a, the three right most strands do not link with the left most string. This shows that the corresponding isotopy class is reducible with a reducing circle containing the three right most strands. Inside this reducing circle the behaviour as a *three* braid is  $\sigma_2 \sigma_1 \sigma_2 \sigma_1 \sigma_2 \sigma_1 = (\sigma_1 \sigma_2)^3$  using the relations in  $B_3$ . This braid is the same as the braid for region D in the planar case, which represents the identity class. Thus for regime X the isotopy classes are reducible with all finite order components. The braid for regime IX is reducible in a way similar to that of regime X, but inside the reducing circle the class is again reducible, but still with all finite order components.

In the braid for regime II shown in Figure 4.4d. The schematic of the plane motion in Figure 4.4b makes it clear that the class is reducible; one can enclose the motions in successive, nested reducing curves. The classes for regime I are similar.

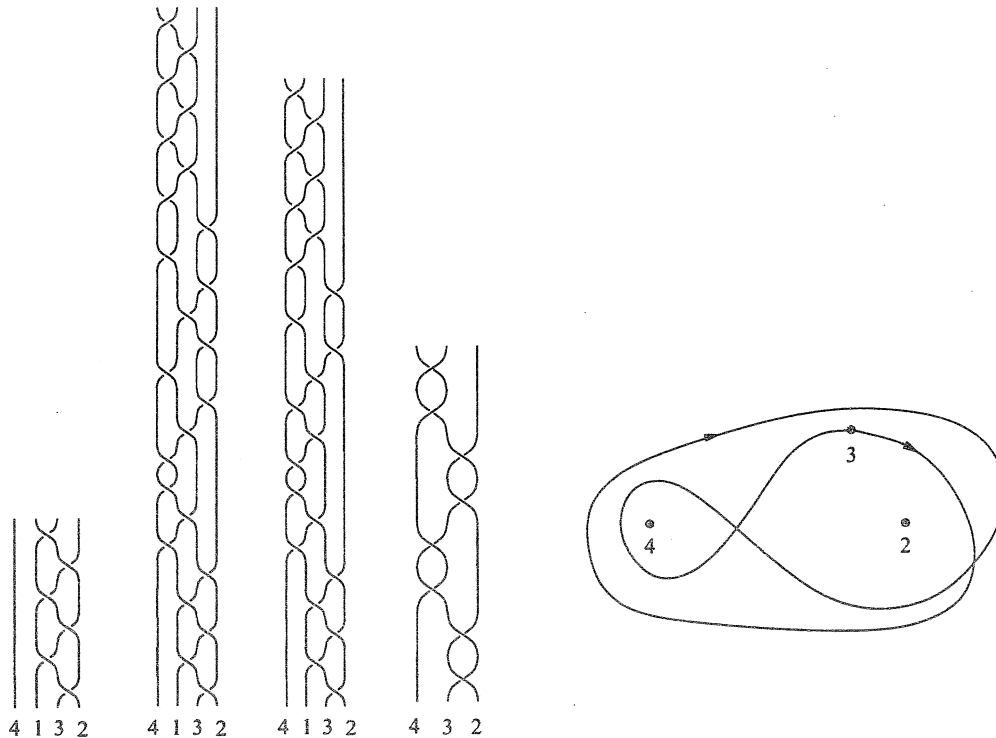


**Figure 6.1:** Mathematical braids of regimes from Figure 3.2: (a) Regime X (b) Regime XII (c) Regime XI. The braid of regime XI restricted to vortices 2, 3, and 4 is shown in (d), and a schematic of the plane motion of the vortices is shown in (e)

The braid for regime XII is shown in Figure 6.1b. The braid makes it clear that vortices 1 and 3 have essentially the same motion with respect to vortex 2 and the origin (“vortex” 4). They do rotate around each other once, but they may be enclosed in a reducing circle. To analyse the class outside the reducing circle we think of squeezing the strands of vortices 1 and 3 into a single strand, or equivalently, we delete one of the strands. The result is the three braid  $\sigma_2^2 \sigma_1^2 \sigma_2^2 \bar{\sigma}_1^2$  shown in Figure 6.1d. This braid corresponds to a pA class rel 3 points with  $\lambda \approx 13.9$ .

Regime XI also yields a pA class with  $\lambda \approx 13.9$ . Although this class is irreducible, the strand corresponding to vortex 1 is in fact a fixed point of the pA map in the class defined by the other three strands. The latter is the same as that for regime XII (see Figure 6.1). The dynamics in regime XI are considered in detail in the next subsection. The last regime is XIII which is pA with  $\lambda \approx 9.9$ .

### §6.3 An example of the dynamical implications of the Thurston-Nielsen theory.

As an example we describe some of the results afforded by the Thurston-Nielsen theory for advection homeomorphisms coming from vortex motions in regime XI. Recall that this regime’s TN-type is pA with  $\lambda \approx 13.9$ . By fixing a periodic orbit  $Z(t)$  in this regime and an initial position  $z_1(0)$  we obtain a motion of all the vortices as in §6.1. The corresponding advection homeomorphism is denoted  $f$ . We may variously consider  $f$  as a homeomorphism of the singly-periodic plane, the cylinder, or as transformed from the cylinder to the plane by the conformal map  $T$ .

Using the theorem of §5.3 and the comments after it we know that the number of fixed points of  $f^n$  grows with  $n$  at least like  $13.9^n$ . These fixed points for  $f^n$  correspond in the lab frame to passive particles that are advected by the vortex velocity field and after  $n$  periods have returned to the same position *relative to the vortices*. They have thus translated by  $nb$ , where  $b$  is the relevant dynamic phase. We also know that under advection, topologically nontrivial curves grow in length at least at a rate of  $13.9^n$ . In addition, the topological entropy of  $f$  is at least  $\log(13.9)$ . This implies that  $f$  has a hyperbolic invariant measure (in the sense of [KH]) with Lyapunov exponents  $\log(13.9)$ , but no information is available regarding its support.

As noted at the end of §4.2, although all the advection homeomorphisms arising from vortex motions in regime XI will have these properties, the time scale of the advection described by the homeomorphism will vary greatly amongst motions in the same regime. In addition, variations in the dynamic phase will make a significant difference in the motion as observed in the lab frame.

The picture of the trajectories of the vortices transformed into the plane is also instructive. Figure 6.1c shows the mathematical braid of this regime. Figure 6.1d shows just the motion of vortices 3 and 2 and the origin (= "vortex" 4), while Figure 6.1e shows a schematic of this motion in the frame of the vortex 2 after it has been transformed to the plane. The feature of note is that the trajectory of vortex 3 crosses itself in an essential way. We cannot remove this self-intersection by deforming the path in the complement of vortex 2 and the origin. This essential self intersection in fact implies that the isotopy class of the advection homeomorphism generated by vortex 3, vortex 2 and the origin is pA. The self-intersection forces regions of the fluid to be repeatedly pushed across pieces of themselves as they are advected. This forces the advection homeomorphism to constantly stretch and fold in an essential topological fashion. It is well known that stretching and folding is a basic mechanism for the generation of chaos and in this case it is topological in nature and is present in any map in the isotopy class.

## §7 Summary and conclusions.

Three-vortex systems with zero net circulation have shown themselves to be worthy of both physical and mathematical interest. Using a combination of dynamical, geometric and topological methods a fairly complete analysis of these systems has been achieved. After fixing a value of the integrals, the reduction process maps the system onto a one degree of freedom Hamiltonian. This Hamiltonian system has a natural subdivision into regimes and we have seen that all the solutions corresponding to a single regime yield topologically identical vortex motions as described by their braids. Viewing the vortices as the "large scale motion" the use of braids allows one to make precise sense of the topology and structure of the large scales. In addition, the notion of reducibility of a braid or isotopy class allows precise description of the hierarchy within the large scale motions. For certain regimes the Thurston-Nielsen theory uses the topology of the vortex motion to obtain very strong conclusions about the advection caused by the large scales. Although point vortices describe a very idealised fluid, it certainly of value to have model systems for which commonly used phrases such as "structure" and "large scale" have a precise meaning with computable implications.

Although this paper has focused on a particular kind of vortex system it should be clear that the methods employed have much wider applicability. Any system involving the periodic motions of points in a surface has a natural description using braids. If there is a natural



homeomorphism on the complement of the points, then it can be studied using Thurston-Nielsen theory. The prototypical such system is an iterated homeomorphism of a surface in which case the collection of points is a collection of periodic orbits. This application is fairly well studied, see [Bd] for a survey. A closely related example is a periodically forced oscillator, see [McT] for a survey. Within fluid mechanics, a two dimensional fluid region with a periodic stirring protocol by rods is studied from this point of view in [BAS].

It is also clear that the methods of this paper apply to a wider class of vortex systems. For example, the methods presented here immediately apply to the periodic motions of  $n > 3$  vortices. However, in the  $n > 3$  case, the reduced dynamics is described by a  $n - 2 > 1$  degree of freedom Hamiltonian system. In this case one expects that the generic bounded orbit is not periodic, but rather only recurrent (via the Poincaré Recurrence Theorem). At a time of near periodicity, such an orbit can be closed in a canonical way and its braid computed. The corresponding advection homeomorphism may then be studied using the Thurston-Nielsen theory. The theoretical task is then to understand how the conclusions derived from the closed motion can be applied to the advection caused by actual recurrent motions. Similar methods could be then applied to the motions of regions of very concentrated vorticity in two-dimensional turbulence and the resulting fluid mixing.

A distinct advantage of the application of the Thurston-Nielsen theory is that it gives quantitative, *a priori* lower bounds for the chaotic dynamics based only on qualitative, topological data. However, the methods are only applicable after a punctured plane is obtained, and then the homeomorphism under question must be in a pseudoAnosov isotopy class. When the methods are applicable an important question is the relative importance of the dynamics dictated by the Thurston-Nielsen theory compared to other sources of chaos. For example, in advection due to point vortices, the singular vorticity gives rise to very violent local stretching. As the vortices move this highly stretched fluid can fold over itself in the classic “chaos engine” scenario. While this effect can be deformed away by an isotopy relative to the vortices, preliminary numerical investigations indicate that in certain cases this effect is an order of magnitude greater than the lower bounds given by Thurston-Nielsen theory. For a smooth distribution of vorticity, this local stretching effect would diminish, and so the global effects given by Thurston-Nielsen theory would presumably gain more importance.

An example where the Thurston-Nielsen effects are clearly dominant is the slow stirring of a viscous fluid studied in [BAS]. Three stirring rods in glycerine were moved in a protocol corresponding to pseudoAnosov braid. Dye tracers indicate an advection dynamics very close to the pA model. The structure of the invariant manifold template of the pA map is clearly visible. The fluid motion in this case seems to realize the least dynamical complexity allowed in its isotopy class which corresponds to very efficient stirring.

The topological methods employed here are very successful in illuminating certain features of the vortex system. As with any method, there are situations of greater and lesser applicability, but when applied with care these topological techniques provide a powerful tool in the study of two-dimensional chaotic dynamics.

## References

- [AR] Adams, M. and Ratiu, T., The three-point vortex problem: commutative and noncommutative integrability, *Contemporary Mathematics*, **81**, 1988, 245–257.



- [Af1] Aref, H., Integrable, chaotic and turbulent vortex motion in two-dimensional flows, *Ann. Rev. Fluid Mech.*, **15**, 1983, 345-389.
- [Af2] Aref, H., Three-vortex motion with zero total circulation: Addendum (Addendum to paper by N. Rott), *J. Appl. Math. Phys. (ZAMP)*, **40**, 1989, 495-500.
- [AS1] Aref, H. and Stremler, M. A., On the motion of three point vortices in a periodic strip, *J. Fluid Mech.*, **314**, 1996, 1-25.
- [AS2] Aref, H. and Stremler, M. A., Vortex quasi-crystals, in preparation.
- [A1] Arnol'd, V. I., Remarks on quasicrystallic symmetries, *Phys. D*, **33**, 1988, 21-25.
- [A2] Arnol'd, V. I., *Mathematical methods of classical mechanics*, Springer-Verlag, 1989.
- [AA] Arnol'd, V. I. and Avez, A., *Ergodic problems of classical mechanics*, Benjamin, 1968.
- [BH] Bestvina, M. and Handel, M., Train tracks for surface homeomorphisms, *Topology*, **34**, 1995, 109-140.
- [Bm1] Birman, J., *Braids, Links and Mapping Class Groups*, Annals of Mathematics Studies, Princeton University Press, 1975.
- [Bm2] Birman, J., On braid groups, *Com. Pure and Appl. Math.*, **22**, 1969, 41-72.
- [BL] Birman, J. and Libgober, A., ed., Proceedings of the AMS-IMS-SIAM Joint Summer Research Conference on Artin's Braid Group, *Contemp. Math.*, **78**, 1988.
- [Bd] Boyland, P. Topological methods in surface dynamics, *Topology and its Applications*, **58**, 223-298, 1994.
- [BAS] Boyland, P., Aref, H. and Stremler, M., Topological fluid mechanics of stirring, *J. Fluid Mech.*, in press.
- [CB] Casson, A. and Bleiler, S., *Automorphisms of Surfaces after Nielsen and Thurston*, London Math. Soc. Stud. Texts, **9**, Cambridge University Press, 1988.
- [C1] Chorin, A. J., Turbulence and vortex stretching on a lattice, *Commun. Pure Appl. Math.*, **39** (Supplement), 1986, S47-S65.
- [C2] Chorin, A. J., Scaling laws in the vortex lattice model of turbulence, *Commun. Math. Phys.*, **114**, 1988, 167-176.
- [C3] Chorin, A. J., Spectrum, dimension, and polymer analogies in fluid turbulence, *Phys. Rev. Lett.*, **60**, 1988, 1947-1949.
- [D] Dugundji, J., *Topology*, Allyn and Bacon, Inc., 1966.
- [FLP] Fathi, A., Lauderbach, F. and Poenaru, V., Travaux de Thurston sur les surfaces, *Asterisque*, **66-67**, 1979.
- [Fk] Franks, J., Anosov diffeomorphisms, *AMS Proceedings of Symposia in Pure Mathematics*, **XIV**, 1970, 61-93.
- [FM2] Franks, J. and Misiurewicz, M., Cycles for disk homeomorphisms and thick trees, *Contemp. Math.*, **152**, 1993, 69-139.
- [H] Handel, M., Global shadowing of pseudo-Anosov homeomorphisms, *Ergod. Th. & Dynam. Sys.*, **5**, 1985, 373-377.
- [J] Janot, C., *Quasicrystals: a primer*, Oxford University Press, 1992.
- [KH] Katok, A. and Hasselblat, B., *Introduction to the modern theory of dynamical systems*, Cambridge University Press, 1995.
- [L] Leonard, A., Computing three-dimensional incompressible flows with vortex elements, *Ann. Rev. Fluid Mech.*, **17**, 1985, 523-559.
- [Ls] Los, J., Pseudo-Anosov maps and invariant train tracks in the disc: a finite algorithm, *Proc. London Math. Soc.*, **66**, 400-430, 1993.

- [McT] McRobie, F. A. and Thompson, J. M. T., Braids and knots in driven oscillators, *Intern. J. Bifurcation & Chaos*, **3**, 1993, 1343–1361.
- [Mj] Majda, A. J., Vorticity, turbulence, and acoustics in fluid flow, *SIAM Rev.*, **33**, 1991, 349–388.
- [M] J. Marsden *Lectures on Mechanics*, LMS Lecture Note Series, **174**, Cambridge University Press, 1992.
- [MZ1] Marsden, J. E., O'Reilly, O. M., Wicklin, F. J., and Zombro, B. W., Symmetry, stability, geometric phases, and mechanical integrators I, *Nonlinear Sci. Today*, **1**, 1991, 4–11.
- [MZ2] Marsden, J. E., O'Reilly, O. M., Wicklin, F. J., and Zombro, B. W., Symmetry, stability, geometric phases, and mechanical integrators II, *Nonlinear Sci. Today*, **2**, 1991, 14–21.
- [MH] Meyer, K.R. and Hall, G.R., *Introduction to Hamiltonian Dynamical Systems and the N-Body Problem*, Springer-Verlag, 1992.
- [MfT] Moffatt, H. K. and Tsinober, A., Helicity in laminar and turbulent flow, *Ann. Rev. Fluid Mech.*, **24**, 1992, 281–312.
- [Mt] Montgomery, R., The  $N$ -body problem, the braid group, and action-minimizing periodic solutions, *Nonlinearity*, **11**, 1998, 363–376.
- [O] O'Neil, K. A., On the Hamiltonian dynamics of vortex lattices, *J. Math. Phys.*, **30**, 1989, 1373–1379.
- [PS] Pullin, D. I. and Saffman, P. G., Vortex dynamics in turbulence, *Ann. Rev. Fluid Mech.*, **30**, 1998, 31–51.
- [R] Roberts, P. H., A Hamiltonian theory for weakly interacting vortices, *Mathematika*, **19**, 1972, 169–179.
- [S] Saffman, P. G., Dynamics of vorticity, *J. Fluid Mech.*, **106**, 1981, 49–58.
- [SB] Saffman, P. G. and Baker, G. R., Vortex interactions, *Ann. Rev. Fluid Mech.*, **11**, 1979, 95–122.
- [Srp] Sarpkaya, T., Computational methods with vortices - The 1988 Freeman Scholar lecture, *J. Fluids Engin.*, **111**, 1989, 5–52.
- [SL] Shariff, K. and Leonard, A., Vortex rings, *Ann. Rev. Fluid Mech.*, **24**, 1992, 235–279.
- [SA] Stremler, M. A. and Aref, H., Motion of three point vortices in a periodic parallelogram, *J. Fluid Mech.*, to appear.
- [T] Thurston, W., On the geometry and dynamics of diffeomorphisms of surfaces, *Bull. A.M.S.*, **19**, 417–431, 1988.
- [Z] Zabusky, N. J., Computational synergetics and mathematical innovation, *J. Comp. Phys.*, **43**, 1981, 195–249.





# List of Recent TAM Reports

| No. | Authors   | Title  | Date       |
|-----|---|--|------------|
| 826 | Riahi, D. N.  | Effects of roughness on nonlinear stationary vortices in rotating disk flows— <i>Mathematical and Computer Modeling</i> 25, 71–82 (1997)   | June 1996  |
| 827 | Riahi, D. N.  | Nonlinear instabilities of shear flows over rough walls, <i>Far East Journal of Applied Mathematics</i> , in press (1998)  | June 1996  |
| 828 | Weaver, R. L.   | Multiple scattering theory for a plate with sprung masses, mean responses— <i>Journal of the Acoustical Society of America</i> 101, 3466–3414 (1997)   | July 1996  |
| 829 | Moser, R. D.,<br>M. M. Rogers, and<br>D. W. Ewing                   | Self-similarity of time-evolving plane wakes <i>Journal of Fluid Mechanics</i> 367, 255–289 (1998)   | July 1996  |
| 830 | Lufrano, J. M., and<br>P. Sofronis                                  | Enhanced hydrogen concentrations ahead of rounded notches and cracks: Competition between plastic strain and hydrostatic stress— <i>Acta Materialia</i> 46, 1519–1526 (1998)                               | July 1996  |
| 831 | Riahi, D. N.  | Effects of surface corrugation on primary instability modes in wall-bounded shear flows  | Aug. 1996  |
| 832 | Bechel, V. T., and<br>N. R. Sottos                                  | Application of debond length measurements to examine the mechanics of fiber pushout, <i>Journal of Mechanics and Physics of Solids</i> 46, 1675–1697 (1998)  | Aug. 1996  |
| 833 | Riahi, D. N.  | Effect of centrifugal and Coriolis forces on chimney convection during alloy solidification— <i>Journal of Crystal Growth</i> 179, 287–296 (1997)  | Sept. 1996 |
| 834 | Cermelli, P., and<br>E. Fried                                       | The influence of inertia on configurational forces in a deformable solid— <i>Proceedings of the Royal Society of London A</i> 453, 1915–1927 (1997)  | Oct. 1996  |
| 835 | Riahi, D. N.  | On the stability of shear flows with combined temporal and spatial imperfections   | Oct. 1996  |
| 836 | Carranza, F. L.,<br>B. Fang, and<br>R. B. Haber                     | An adaptive space-time finite element model for oxidation-driven fracture, <i>Computer Methods in Applied Mechanics and Engineering</i> , in press (1997)  | Nov. 1996  |
| 837 | Carranza, F. L.,<br>B. Fang, and<br>R. B. Haber                     | A moving cohesive interface model for fracture in creeping materials, <i>Computational Mechanics</i> 19, 517–521 (1997)  | Nov. 1996  |
| 838 | Balachandar, S.,<br>R. Mittal, and<br>F. M. Najjar                  | Properties of the mean wake recirculation region in two-dimensional bluff body wakes— <i>Journal of Fluid Mechanics</i> , in press (1997)  | Dec. 1996  |
| 839 | Ti, B. W.,<br>W. D. O'Brien, Jr., and<br>J. G. Harris               | Measurements of coupled Rayleigh wave propagation in an elastic plate— <i>Journal of the Acoustical Society of America</i> 102, 1528–1531  | Dec. 1996  |
| 840 | Phillips, W. R. C.  | On finite-amplitude rotational waves in viscous shear flows— <i>Studies in Applied Mathematics</i> 100, in press (1998)  | Jan. 1997  |
| 841 | Riahi, D. N.  | Direct resonance analysis and modeling for a turbulent boundary layer over a corrugated surface— <i>Acta Mechanica</i> , in press (1998)   | Jan. 1997  |
| 842 | Liu, Z.-C., R. J. Adrian,<br>C. D. Meinhart, and<br>W. Lai          | Structure of a turbulent boundary layer using a stereoscopic, large format video-PIV— <i>Developments in Laser Techniques and Fluid Mechanics</i> , 259–273 (1997)   | Jan. 1997  |
| 843 | Fang, B.,<br>F. L. Carranza, and<br>R. B. Haber                     | An adaptive discontinuous Galerkin method for viscoplastic analysis— <i>Computer Methods in Applied Mechanics and Engineering</i> 150, 191–198 (1997)  | Jan. 1997  |
| 844 | Xu, S., T. D. Aslam,<br>and D. S. Stewart                           | High-resolution numerical simulation of ideal and non-ideal compressible reacting flows with embedded internal boundaries— <i>Combustion Theory and Modeling</i> 1, 113–142 (1997)                         | Jan. 1997  |
| 845 | Zhou, J.,<br>C. D. Meinhart,<br>S. Balachandar, and<br>R. J. Adrian | Formation of coherent hairpin packets in wall turbulence—In <i>Self-Sustaining Mechanisms in Wall Turbulence</i> , R. L. Panton, ed. Southampton, UK: Computational Mechanics Publications, 109–134 (1997) | Feb. 1997  |

# List of Recent TAM Reports (cont'd)

| No. | Authors   | Title  | Date       |
|-----|---|--|------------|
| 846 | Lufrano, J. M.,<br>P. Sofronis, and<br>H. K. Birnbaum           | Elastoplastically accommodated hydride formation and embrittlement— <i>Journal of Mechanics and Physics of Solids</i> , in press (1998)  | Feb. 1997  |
| 847 | Keane, R. D.,<br>N. Fujisawa, and<br>R. J. Adrian               | Unsteady non-penetrative thermal convection from non-uniform surfaces—In <i>Geophysical and Astrophysical Convection</i> , R. Kerr, ed. (1997)   | Feb. 1997  |
| 848 | Aref, H., and M. Brøns  | On stagnation points and streamline topology in vortex flows— <i>Journal of Fluid Mechanics</i> <b>370</b> , 1–27 (1998)   | Mar. 1997  |
| 849 | Asghar, S., T. Hayat,<br>and J. G. Harris                       | Diffraction by a slit in an infinite porous barrier— <i>Wave Motion</i> , in press (1998)  | Mar. 1997  |
| 850 | Shawki, T. G., H. Aref,<br>and J. W. Phillips                   | Mechanics on the Web—Proceedings of the International Conference on Engineering Education (Aug. 1997, Chicago)   | Apr. 1997  |
| 851 | Stewart, D. S., and<br>J. Yao                                   | The normal detonation shock velocity-curvature relationship for materials with non-ideal equation of state and multiple turning points— <i>Combustion</i> <b>113</b> , 224–235 (1998)  | Apr. 1997  |
| 852 | Fried, E., A. Q. Shen,<br>and S. T. Thoroddsen                  | Wave patterns in a thin layer of sand within a rotating horizontal cylinder— <i>Physics of Fluids</i> <b>10</b> , 10–12 (1998)   | Apr. 1997  |
| 853 | Boyland, P. L., H. Aref,<br>and M. A. Stremler                  | Topological fluid mechanics of stirring— <i>Bulletin of the American Physical Society</i> <b>41</b> , 1683 (1996)  | Apr. 1997  |
| 854 | Parker, S. J., and<br>S. Balachandar                            | Viscous and inviscid instabilities of flow along a streamwise corner— <i>Bulletin of the American Physical Society</i> <b>42</b> , 2155 (1997)   | May 1997   |
| 855 | Soloff, S. M.,<br>R. J. Adrian, and<br>Z.-C. Liu                | Distortion compensation for generalized stereoscopic particle image velocimetry— <i>Measurement Science and Technology</i> <b>8</b> , 1–14 (1997)  | May 1997   |
| 856 | Zhou, Z., R. J. Adrian,<br>S. Balachandar, and<br>T. M. Kendall | Mechanisms for generating coherent packets of hairpin vortices in near-wall turbulence— <i>Bulletin of the American Physical Society</i> <b>42</b> , 2243 (1997)   | June 1997  |
| 857 | Neishtadt, A. I.,<br>D. L. Vainshtein, and<br>A. A. Vasiliev    | Chaotic advection in a cubic stokes flow— <i>Physica D</i> <b>111</b> , 227 (1997).  | June 1997  |
| 858 | Weaver, R. L.   | Ultrasonics in an aluminum foam— <i>Ultrasonics</i> <b>36</b> , 435–442 (1998)   | July 1997  |
| 859 | Riahi, D. N.  | High gravity convection in a mushy layer during alloy solidification—In <i>Nonlinear Instability, Chaos and Turbulence</i> , D. N. Riahi and L. Debnath, eds., in press (1998)   | July 1997  |
| 860 | Najjar, F. M., and<br>S. Balachandar                            | Low-frequency unsteadiness in the wake of a normal plate, <i>Bulletin of the American Physical Society</i> <b>42</b> , 2212 (1997)   | Aug. 1997  |
| 861 | Short, M.   | A parabolic linear evolution equation for cellular detonation instability— <i>Combustion Theory and Modeling</i> <b>1</b> , 313–346 (1997)   | Aug. 1997  |
| 862 | Short, M., and<br>D. S. Stewart                                 | Cellular detonation stability, I: A normal-mode linear analysis— <i>Journal of Fluid Mechanics</i> <b>368</b> , 229–262 (1998)   | Sept. 1997 |
| 863 | Carranza, F. L., and<br>R. B. Haber                             | A numerical study of intergranular fracture and oxygen embrittlement in an elastic-viscoplastic solid— <i>Journal of the Mechanics and Physics of Solids</i> , in press (1997)   | Oct. 1997  |
| 864 | Sakakibara, J., and<br>R. J. Adrian                             | Whole-field measurement of temperature in water using two-color laser-induced fluorescence— <i>Experiments in Fluids</i> <b>26</b> , 7–15 (1999)   | Oct. 1997  |
| 865 | Riahi, D. N.  | Effect of surface corrugation on convection in a three-dimensional finite box of fluid-saturated porous material   | Oct. 1997  |
| 866 | Baker, C. F., and<br>D. N. Riahi                                | Three-dimensional flow instabilities during alloy solidification   | Oct. 1997  |
| 867 | Fried, E.   | Introduction (only) to <i>The Physical and Mathematical Foundations of the Continuum Theory of Evolving Phase Interfaces</i> (book containing 14 seminal papers dedicated to Morton E. Gurtin), Berlin: Springer-Verlag, in press (1998) | Oct. 1997  |
| 868 | Folguera, A., and<br>J. G. Harris                               | Coupled Rayleigh surface waves in a slowly varying elastic waveguide— <i>Proceedings of the Royal Society of London</i> , in press (1998)  | Oct. 1997  |

# List of Recent TAM Reports (cont'd)

| No. | Authors                                     | Title   | Date       |
|-----|---|---|------------|
| 869 | Stewart, D. S.                              | Detonation shock dynamics: Application for precision cutting of metal with detonation waves   | Oct. 1997  |
| 870 | Shrotriya, P., and N. R. Sottos             | Creep and relaxation behavior of woven glass/epoxy substrates for multilayer circuit board applications— <i>Polymer Composites</i> 19, 567–578 (1998)                             | Nov. 1997  |
| 871 | Riahi, D. N.                                | Boundary wave–vortex interaction in channel flow at high Reynolds numbers, <i>Fluid Dynamics Research</i> 25, 129–145 (1999)  | Nov. 1997  |
| 872 | George, W. K., L. Castillo, and M. Wosnik   | A theory for turbulent pipe and channel flows—paper presented at <i>Disquisitiones Mechanicae</i> (Urbana, Ill., October 1996)  | Nov. 1997  |
| 873 | Aslam, T. D., and D. S. Stewart             | Detonation shock dynamics and comparisons with direct numerical simulation— <i>Combustion Theory and Modeling</i> , in press (1999)   | Dec. 1997  |
| 874 | Short, M., and A. K. Kapila                 | Blow-up in semilinear parabolic equations with weak diffusion   | Dec. 1997  |
| 875 | Riahi, D. N.                                | Analysis and modeling for a turbulent convective plume— <i>Mathematical and Computer Modeling</i> 28, 57–63 (1998)  | Jan. 1998  |
| 876 | Stremmer, M. A., and H. Aref                | Motion of three point vortices in a periodic parallelogram— <i>Journal of Fluid Mechanics</i> , in press (1999)   | Feb. 1998  |
| 877 | Dey, N., K. J. Hsia, and D. F. Socie        | On the stress dependence of high-temperature static fatigue life of ceramics  | Feb. 1998  |
| 878 | Brown, E. N., and N. R. Sottos              | Thermoelastic properties of plain weave composites for multilayer circuit board applications  | Feb. 1998  |
| 879 | Riahi, D. N.                                | On the effect of a corrugated boundary on convective motion— <i>Journal of Theoretical and Applied Mechanics</i> , in press (1999)  | Feb. 1998  |
| 880 | Riahi, D. N.                                | On a turbulent boundary layer flow over a moving wavy wall  | Mar. 1998  |
| 881 | Riahi, D. N.                                | Vortex formation and stability analysis for shear flows over combined spatially and temporally structured walls   | June 1998  |
| 882 | Short, M., and D. S. Stewart                | The multi-dimensional stability of weak heat release detonations  | June 1998  |
| 883 | Fried, E., and M. E. Gurtin                 | Coherent solid-state phase transitions with atomic diffusion: A thermomechanical treatment— <i>Journal of Statistical Physics</i> , in press (1999)                               | June 1998  |
| 884 | Langford, J. A., and R. D. Moser            | Optimal large-eddy simulation formulations for isotropic turbulence   | July 1998  |
| 885 | Riahi, D. N.                                | Boundary-layer theory of magnetohydrodynamic turbulent convection— <i>Proceedings of the Indian National Academy (Physical Science)</i> , in press (1999)                         | Aug. 1998  |
| 886 | Riahi, D. N.                                | Nonlinear thermal instability in spherical shells—in <i>Nonlinear Instability, Chaos and Turbulence</i> 2, in press (1999)  | Aug. 1998  |
| 887 | Riahi, D. N.                                | Effects of rotation on fully non-axisymmetric chimney convection during alloy solidification— <i>Journal of Crystal Growth</i> 204, 382–394 (1999)                                | Sept. 1998 |
| 888 | Fried, E., and S. Sellers                   | The Debye theory of rotary diffusion  | Sept. 1998 |
| 889 | Short, M., A. K. Kapila, and J. J. Quirk    | The hydrodynamic mechanisms of pulsating detonation wave instability  | Sept. 1998 |
| 890 | Stewart, D. S.                              | The shock dynamics of multidimensional condensed and gas phase detonations—Proceedings of the 27th International Symposium on Combustion (Boulder, Colo.)                         | Sept. 1998 |
| 891 | Kim, K. C., and R. J. Adrian                | Very large-scale motion in the outer layer  | Oct. 1998  |
| 892 | Fujisawa, N., and R. J. Adrian              | Three-dimensional temperature measurement in turbulent thermal convection by extended range scanning liquid crystal thermometry   | Oct. 1998  |
| 893 | Shen, A. Q., E. Fried, and S. T. Thoroddsen | Is segregation-by-particle-type a generic mechanism underlying finger formation at fronts of flowing granular media?— <i>Particulate Science and Technology</i> , in press (1999) | Oct. 1998  |

# **List of Recent TAM Reports (cont'd)**

| <i>No.</i> | <i>Authors</i>  | <i>Title</i>   | <i>Date</i> |
|------------|---|--|-------------|
| 894        | Shen, A. Q.   | Mathematical and analog modeling of lava dome growth   | Oct. 1998   |
| 895        | Buckmaster, J. D., and M. Short                           | Cellular instabilities, sub-limit structures, and edge-flames in premixed counterflows   | Oct. 1998   |
| 896        | Harris, J. G.   | <i>Elastic waves</i> —Part of a book to be published by Cambridge University Press   | Dec. 1998   |
| 897        | Paris, A. J., and G. A. Costello                          | Cord composite cylindrical shells  | Dec. 1998   |
| 898        | Students in TAM 293–294                                   | Thirty-fourth student symposium on engineering mechanics (May 1997), J. W. Phillips, coordinator: Selected senior projects by M. R. Bracki, A. K. Davis, J. A. (Myers) Hommema, and P. D. Pattillo | Dec. 1998   |
| 899        | Taha, A., and P. Sofronis                                 | A micromechanics approach to the study of hydrogen transport and embrittlement   | Jan. 1999   |
| 900        | Ferney, B. D., and K. J. Hsia                             | The influence of multiple slip systems on the brittle–ductile transition in silicon  | Feb. 1999   |
| 901        | Fried, E., and A. Q. Shen                                 | Supplemental relations at a phase interface across which the velocity and temperature jump   | Mar. 1999   |
| 902        | Paris, A. J., and G. A. Costello                          | Cord composite cylindrical shells: Multiple layers of cords at various angles to the shell axis  | Apr. 1999   |
| 903        | Ferney, B. D., M. R. DeVary, K. J. Hsia, and A. Needleman | Oscillatory crack growth in glass  | Apr. 1999   |
| 904        | Fried, E., and S. Sellers                                 | Microforces and the theory of solute transport   | Apr. 1999   |
| 905        | Balachandar, S., J. D. Buckmaster, and M. Short           | The generation of axial vorticity in solid-propellant rocket-motor flows   | May 1999    |
| 906        | Aref, H., and D. L. Vainchtein                            | The equation of state of a foam  | May 1999    |
| 907        | Subramanian, S. J., and P. Sofronis                       | Modeling of the interaction between densification mechanisms in powder compaction  | May 1999    |
| 908        | Aref, H., and M. A. Stremler                              | Four-vortex motion with zero total circulation and impulse   | May 1999    |
| 909        | Adrian, R. J., K. T. Christensen, and Z.-C. Liu           | On the analysis and interpretation of turbulent velocity fields  | May 1999    |
| 910        | Fried, E., and S. Sellers                                 | Theory for atomic diffusion on fixed and deformable crystal lattices   | June 1999   |
| 911        | Sofronis, P., and N. Aravas                               | Hydrogen induced shear localization of the plastic flow in metals and alloys   | June 1999   |
| 912        | Anderson, D. R., D. E. Carlson, and E. Fried              | A continuum-mechanical theory for nematic elastomers   | June 1999   |
| 913        | Riahi, D. N.  | High Rayleigh number convection in a rotating melt during alloy solidification   | July 1999   |
| 914        | Riahi, D. N.  | Buoyancy driven flow in a rotating low Prandtl number melt during alloy solidification   | July 1999   |
| 915        | Adrian, R. J.   | On the physical space equation for large-eddy simulation of inhomogeneous turbulence   | July 1999   |
| 916        | Riahi, D. N.  | Wave and vortex generation and interaction in turbulent channel flow between wavy boundaries   | July 1999   |
| 917        | Boyland, P. L., M. A. Stremler, and H. Aref               | Topological fluid mechanics of point vortex motions  | July 1999   |